# Light-induced $O_2$-dependent aliphatic carbon-carbon (C-C) bond cleavage in bipyridine-ligated Co(II) chlorodiketonate complexes

Stephen N. Anderson[†], Josiah G. D. Elsberg[†], and Lisa M. Berreau*[,†]

[†]Department of Chemistry and Biochemistry, Utah State University, Logan, Utah 84322-0300, United States

**Table of Contents** **Page**

**Table S1.** Summary of X-ray data collection and refinement.[a]

| | **8 • $O(CH_2CH_3)_2$** | **9 • 0.5 $CH_3CN$ • 0.5 $O(CH_2CH_3)_2$** | **10** | **12** |
|---|---|---|---|---|
| Empirical formula | $C_{39}H_{36}Cl_2CoN_4O_7$ | $C_{40}H_{36.5}Cl_2CoN_{4.5}O_{6.5}$ | $C_{37}H_{30}Cl_2CoN_4O_8$ | $C_{24}H_{22}Cl_2CoN_6O_8$ |
| Formula weight | 802.55 | 814.06 | 788.48 | 652.30 |
| Crystal system | Triclinic | Orthorhombic | Monoclinic | Triclinic |
| Space group | P-1 | $Pna2_1$ | $P2_1/n$ | P-1 |
| *a* (Å) | 11.3963(6) | 21.4753(12) | 13.8215(7) | 10.0272(8) |
| *b* (Å) | 12.6001(7) | 17.7824(9) | 18.0740(10) | 10.2270(6) |
| *c* (Å) | 14.2773(7) | 19.6340(12) | 14.7453(7) | 15.4354(6) |
| α (deg) | 73.724(2) | 90 | 90 | 83.304(4) |
| β (deg) | 86.205(2) | 90 | 110.426(2) | 83.219(4) |
| γ (deg) | 69.356(2) | 90 | 90 | 61.217(7) |
| V ($Å^3$) | 1840.40(17) | 7497.9(7) | 3451.9(3) | 1372.19(17) |
| Z | 2 | 8 | 4 | 2 |
| $\rho_{calc}$ ($g/cm^3$) | 1.448 | 1.442 | 1.517 | 1.579 |
| Temp (K) | 100 | 100 | 100 | 100 |
| Crystal size ($mm^{-1}$) | 0.28 × 0.226 × 0.11 | 0.24 × 0.21 × 0.20 | 0.26 × 0.25 × 0.02 | 0.24 × 0.19 ×0.12 |
| Diffractometer | Bruker D8 Venture | Bruker D8 Venture | Bruker D8 Venture | Rigaku XtaLAB Mini II Diffractometer |
| Abs. coeff. ($mm^{-1}$) | 0.668 | 0.656 | 0.712 | 0.879 |
| 2θ (deg) | 54.298 | 55.162 | 55.1 | 60.234 |
| Reflections collected | 87249 | 96371 | 54870 | 25701 |
| Indep. Reflections | 8151 | 17244 | 7949 | 8973 |
| *R*1 / w*R*2[b] | 0.0411 / 0.1019 | 0.0356 / 0.0837 | 0.0352 / 0.0736 | 0.0363 / 0.0885 |
| GOF ($F^2$) | 1.047 | 1.032 | 1.027 | 1.042 |
| $\Delta\rho_{max}$ / $\Delta\rho_{min}$ (e $Å^{-3}$) | 1.0 / -0.7 | 0.61 / -0.26 | 0.58 / -0.41 | 0.47 / -0.49 |

[a] Radiation used: MoKα (λ = 0.71073 Å). [b] $R1 = \sum||F_o| - |F_c||/\sum|F_o|$; $wR2 = [\sum[w(F_o^2 - F_c^2)^2]/[\sum(F_o^2)^2]]^{1/2}$ where $w = 1/[\sigma^2(F_o^2) + (aP)^2 + bP]$.

**Table S2.** Selected bond distances (Å) for **8**-**10**

| | **8** | **9A** | **9B** | **10** |
|---|---|---|---|---|
| Co(1)-O(1) | 2.0596(14) | 2.034(3) | 2.024(3) | 2.0577(13) |
| Co(1)-O(2) | 2.0437(15) | 2.030(2) | 2.027(2) | 2.0286(13) |
| Co(1)-N(1) | 2.1333(17) | 2.146(3) | 2.134(3) | 2.1544(16) |
| Co(1)-N(2) | 2.1251(17) | 2.152(3) | 2.139(3) | 2.1040(15) |
| Co(1)-N(3) | 2.1136(17) | 2.114(3) | 2.110(3) | 2.1307(16) |
| Co(1)-N(4) | 2.1321(18) | 2.109(3) | 2.106(3) | 2.1269(16) |
| O(1)-C(22) | 1.267(2) | 1.260(4) | 1.280(4) | 1.272(2) |
| O(2)-C(21) | 1.265(3) | 1.262(4) | 1.262(4) | 1.267(2) |
| C(21)-C(23) | 1.404(3) | 1.412(5) | 1.420(5) | 1.413(3) |
| C(22)-C(23) | 1.414(3) | 1.406(5) | 1.411(5) | 1.412(3) |

**Table S3.** Selected bond angles (deg) for **8**-**10**

| | **8** | **9A** | **9B** | **10** |
|---|---|---|---|---|
| O(1)-Co(1)-N(1) | 171.12(6) | 168.96(10) | 86.70(10) | 162.39(6) |
| O(1)-Co(1)-N(2) | 96.60(6) | 92.73(11) | 170.22(11) | 93.02(6) |
| O(1)-Co(1)-N(3) | 92.08(6) | 97.44(11) | 94.03(12) | 91.67(6) |
| O(1)-Co(1)-N(4) | 87.37(6) | 89.61(11) | 93.29(12) | 94.73(5) |
| O(2)-Co(1)-O(1) | 86.02(6) | 86.70(10) | 92.88(11) | 85.80(5) |
| O(2)-Co(1)-N(1) | 87.80(6) | 89.36(10) | 89.47(11) | 81.29(6) |
| O(2)-Co(1)-N(2) | 89.04(6) | 87.42(11) | 89.19(11) | 97.13(6) |
| O(2)-Co(1)-N(3) | 95.97(6) | 93.09(11) | 94.63(11) | 90.26(6) |
| O(2)-Co(1)-N(4) | 170.14(6) | 168.98(11) | 171.70(11) | 167.23(6) |
| N(2)-Co(1)-N(1) | 76.91(7) | 76.79(12) | 76.90(12) | 76.85(6) |
| N(2)-Co(1)-N(4) | 98.99(7) | 103.14(12) | 95.99(12) | 95.58(6) |
| N(3)-Co(1)-N(1) | 94.90(7) | 93.06(12) | 92.19(11) | 100.28(6) |
| N(3)-Co(1)-N(2) | 170.26(7) | 169.83(13) | 171.93(12) | 171.51(6) |
| N(3)-Co(1)-N(4) | 76.96(7) | 77.09(12) | 77.11(12) | 76.98(6) |
| N(4)-Co(1)-N(1) | 99.54(7) | 96.06(11) | 99.11(12) | 100.51(6) |
| C(22)-O(1)-Co(1) | 128.50(13) | 127.9(2) | 129.4(2) | 128.22(12) |
| C(21)-O(2)Co(1) | 127.21(14) | 129.3(2) | 130.7(2) | 131.73(12) |
| O(1)-C(22)-C(23) | 123.45(19) | 124.5(3) | 123.8(3) | 124.29(17) |
| O(2)-C(21)-C(23) | 124.3(2) | 123.2(3) | 122.9(3) | 121.59(16) |
| O(1)-C(22)-C(25) | 115.39(18) | 114.3(3) | 114.1(3) | 115.70(15) |
| O(2)-C(21)-C(24) | 114.95(19) | 114.1(3) | 114.6(3) | 114.49(16) |
| C(21)-C(23)-C(22) | 124.82(19) | 124.7(3) | 124.8(3) | 125.15(17) |
| C(23)-C(21)-C(24) | 120.75(19) | 122.6(3) | 122.5(3) | 123.86(16) |
| C(23)-C(22)-C(25) | 121.14(19) | 121.1(3) | 122.1(3) | 119.96(16) |

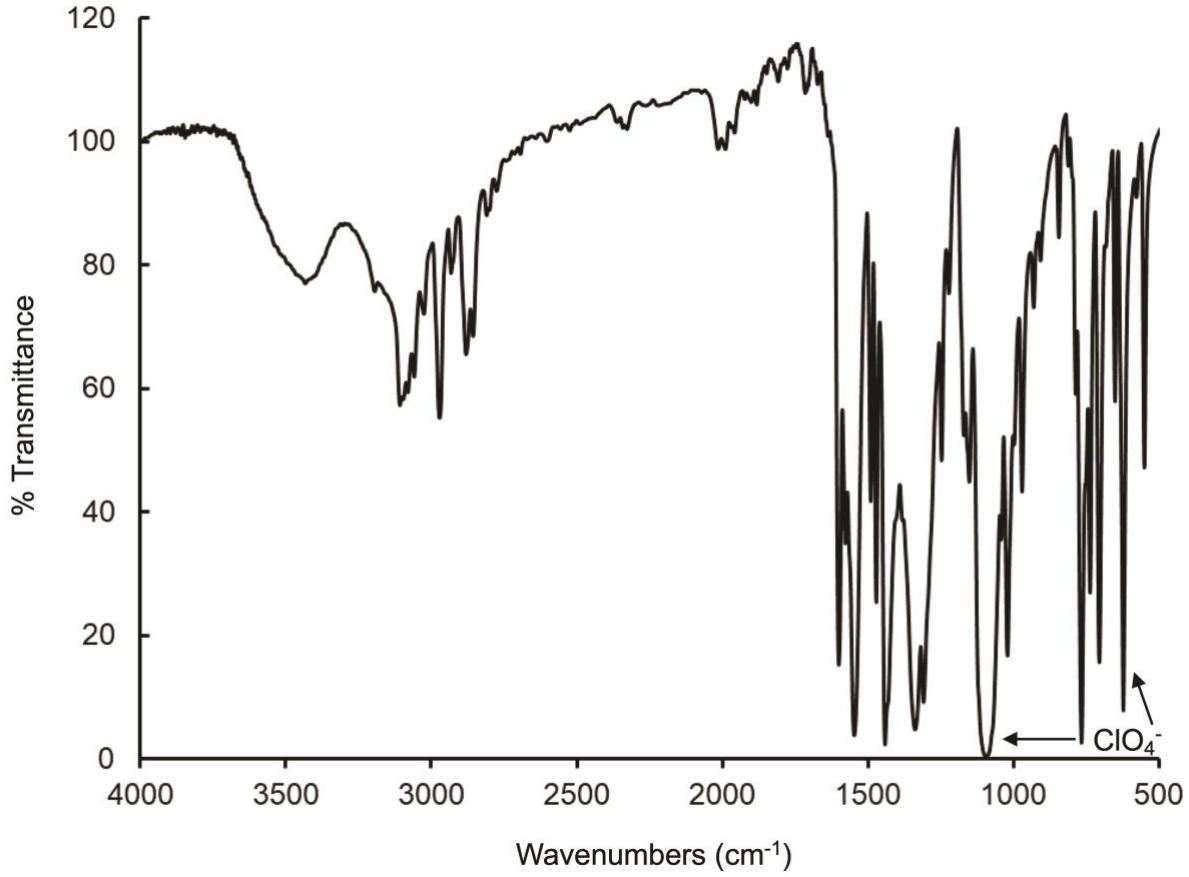


**Fig S1.** FTIR spectrum for **8** collected as a KBr pellet.

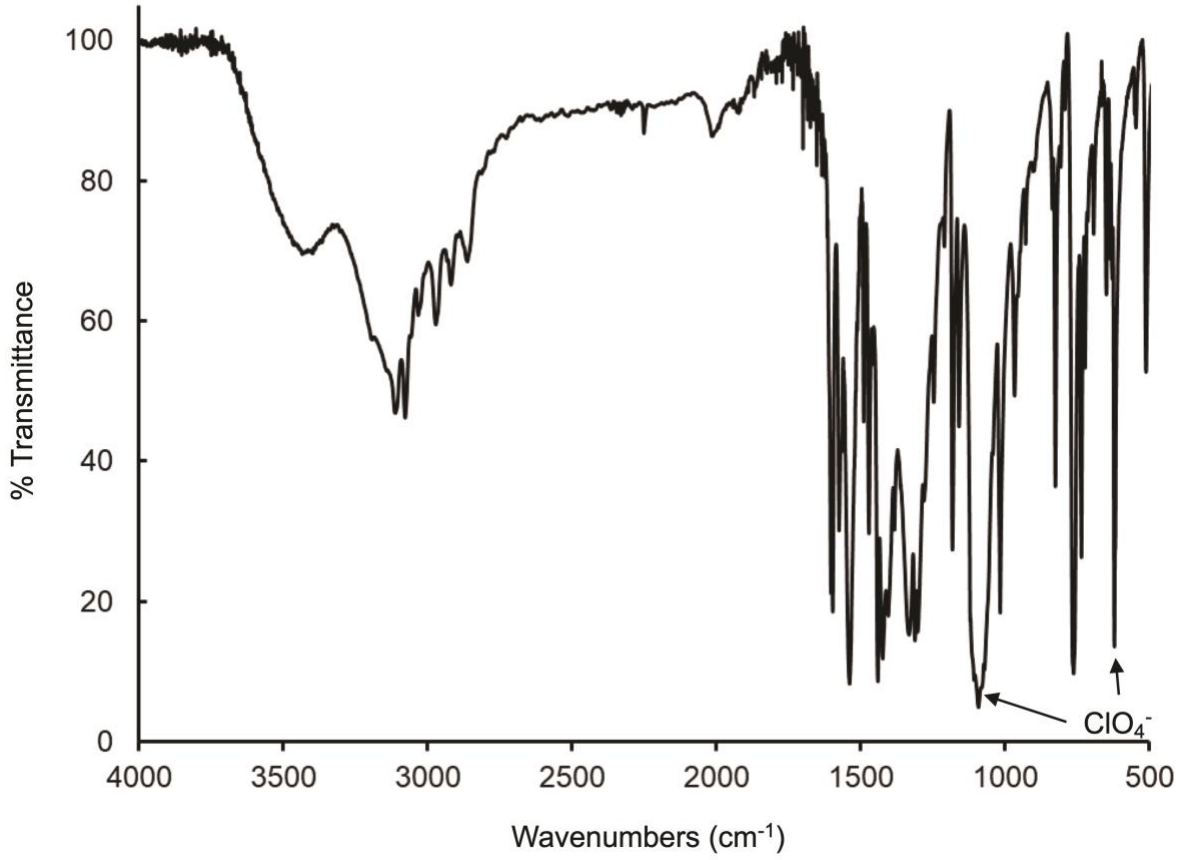


**Fig S2.** FTIR spectrum for **9** collected as a KBr pellet.

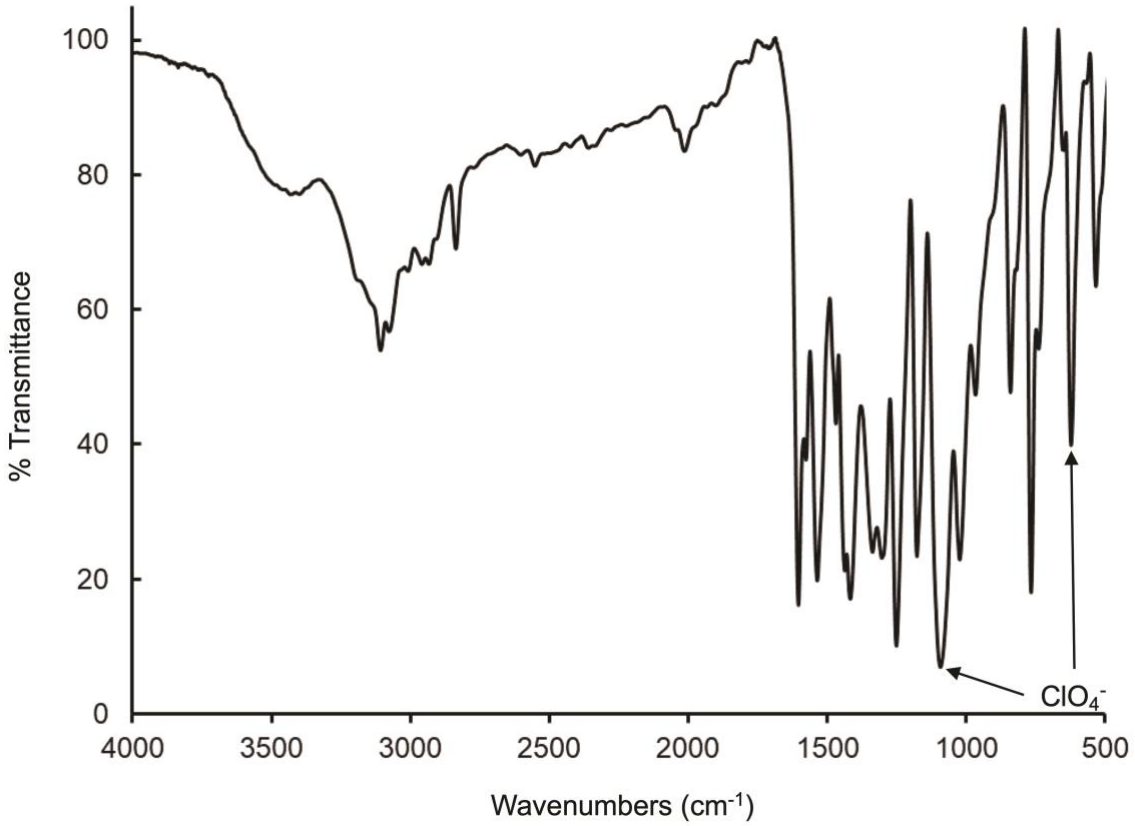


**Fig S3.** IR spectrum for **10** collected as a KBr pellet.

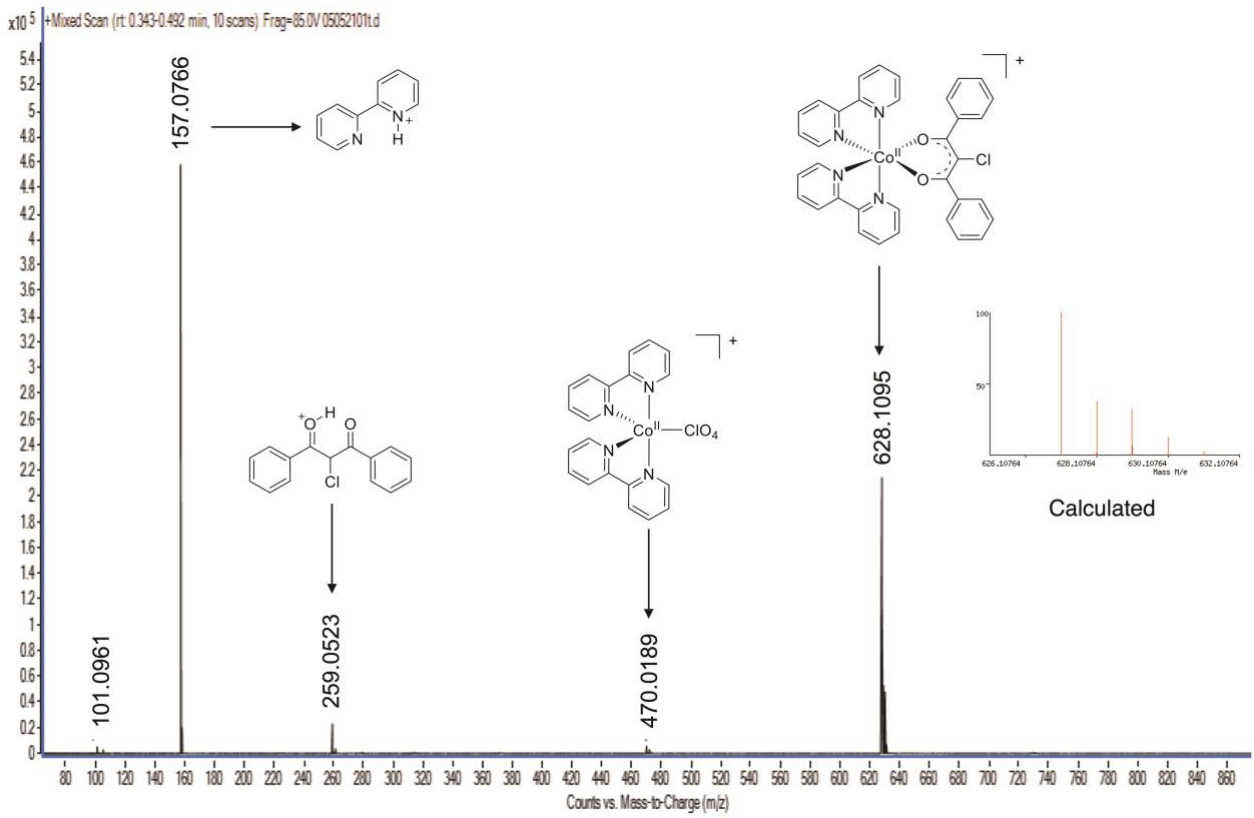


**Fig S4.** ESI-MS of **8** in $CH_3CN$.

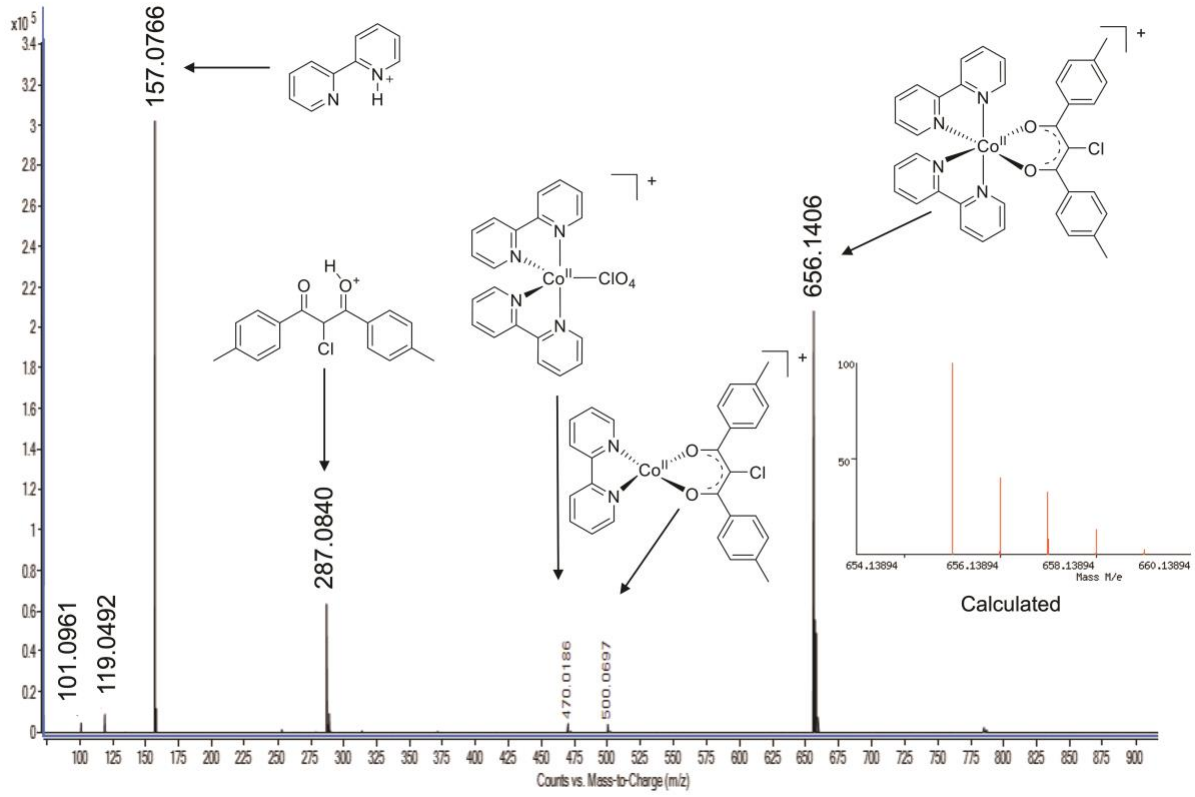


**Fig S5.** ESI-MS of **9** in $CH_3CN$.

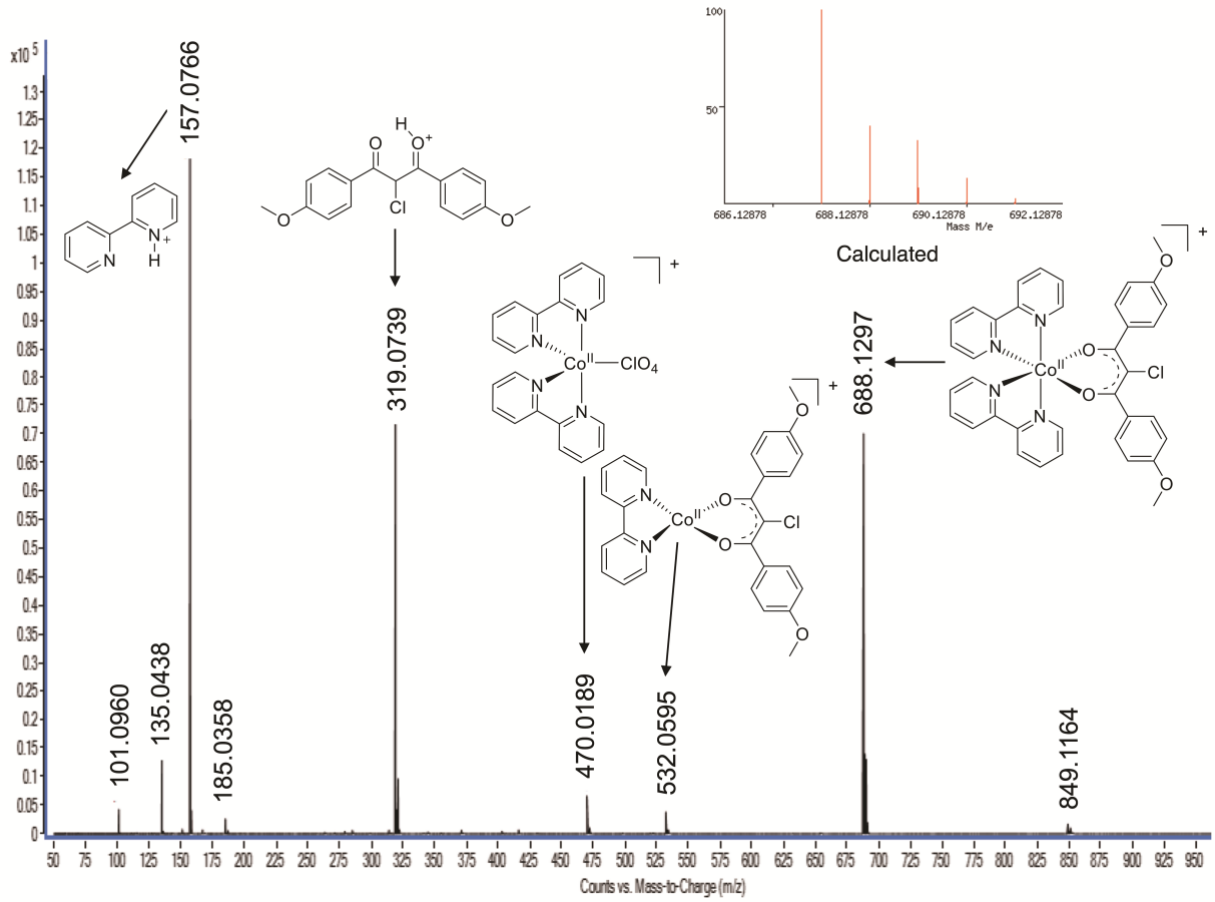


**Fig S6.** ESI-MS of **10** in $CH_3CN$.

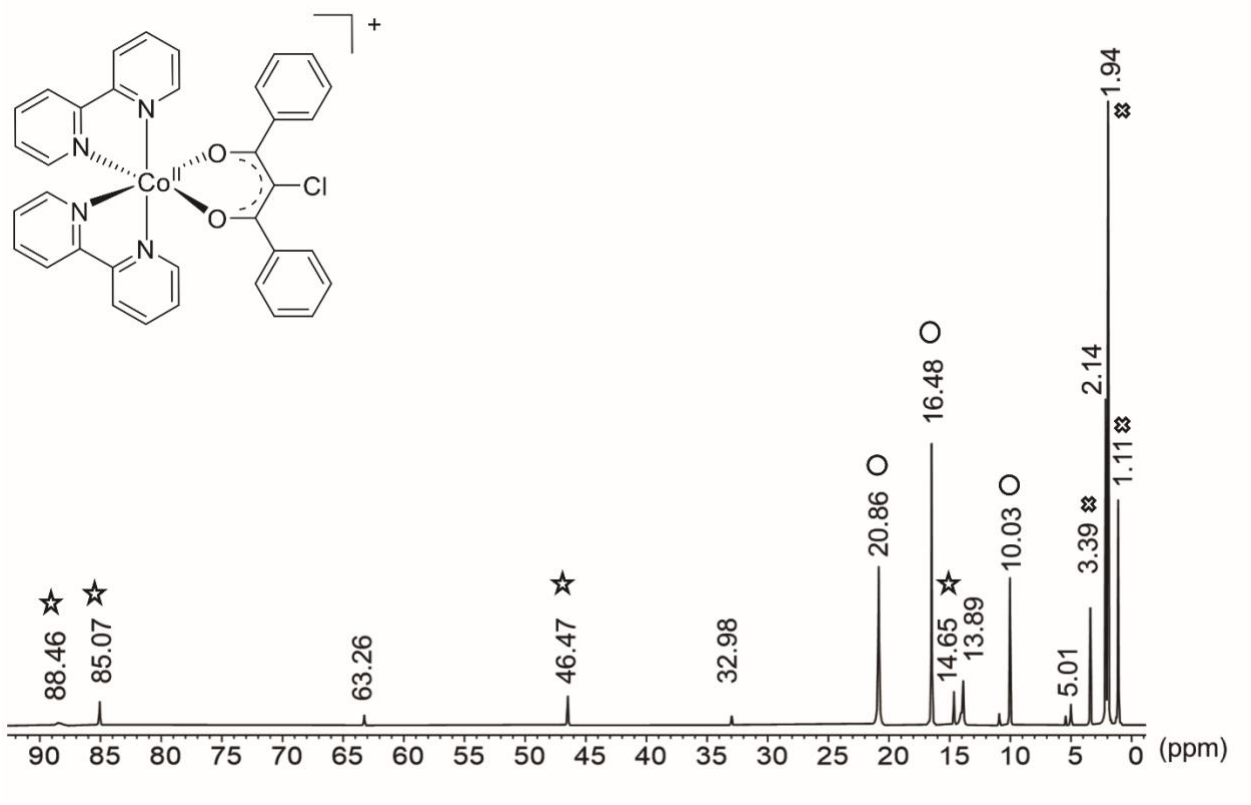


**Fig S7.** $^{1}$H NMR of **8** in $CD_3CN$. The signals marked with an open circle correspond to the coordinated diketonate ligand in **8**. Signals marked with a star indicate those from $[(bpy)_3Co](ClO_4)_2$ (**11**). Residual solvent signals are indicated with (X).

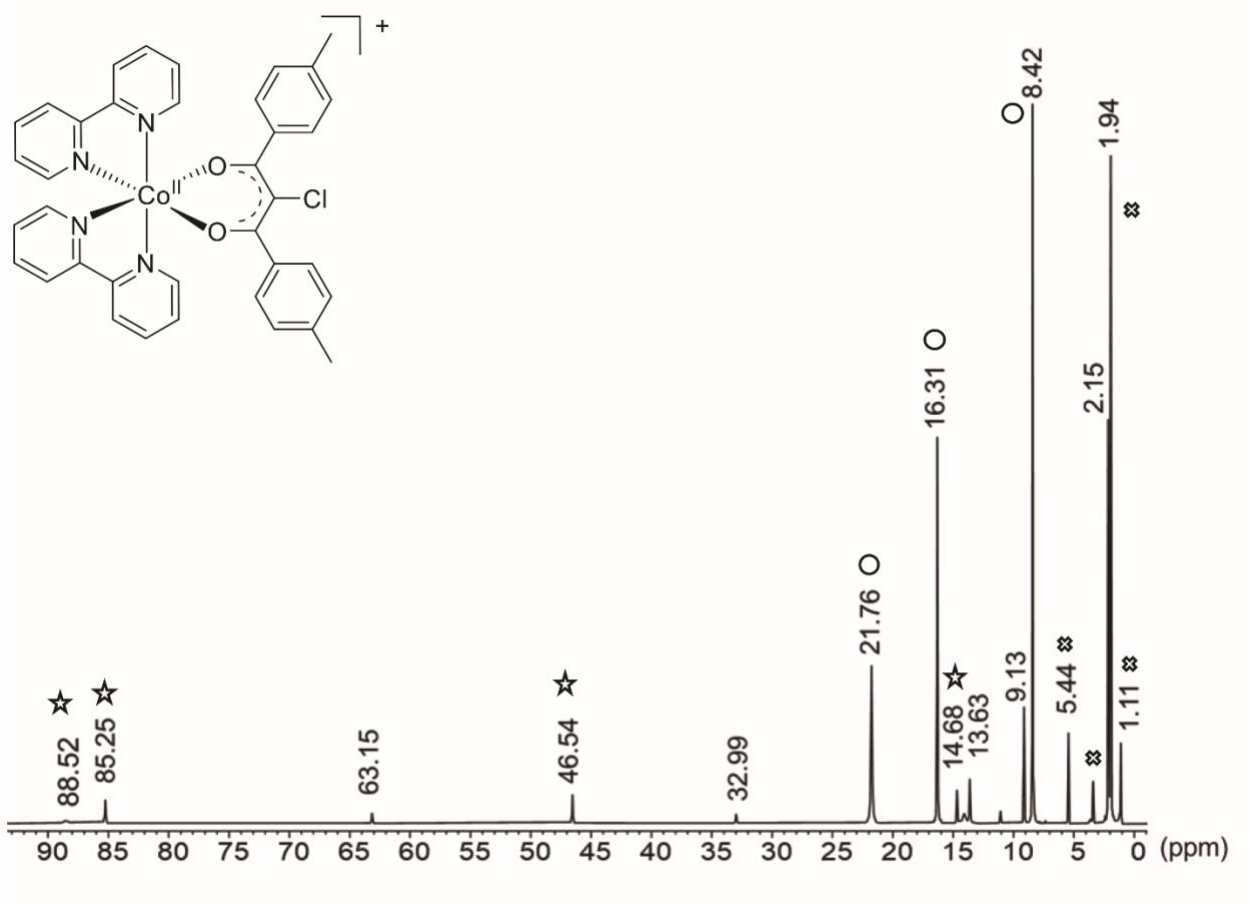


**Fig S8.** $^{1}$H NMR of **9** in $CD_3CN$. The signals marked with an open circle correspond to the coordinated diketonate ligand in **9**. Signals marked with a star indicate those from $[(bpy)_3Co](ClO_4)_2$ (**11**). Residual solvent signals are indicated with (X).

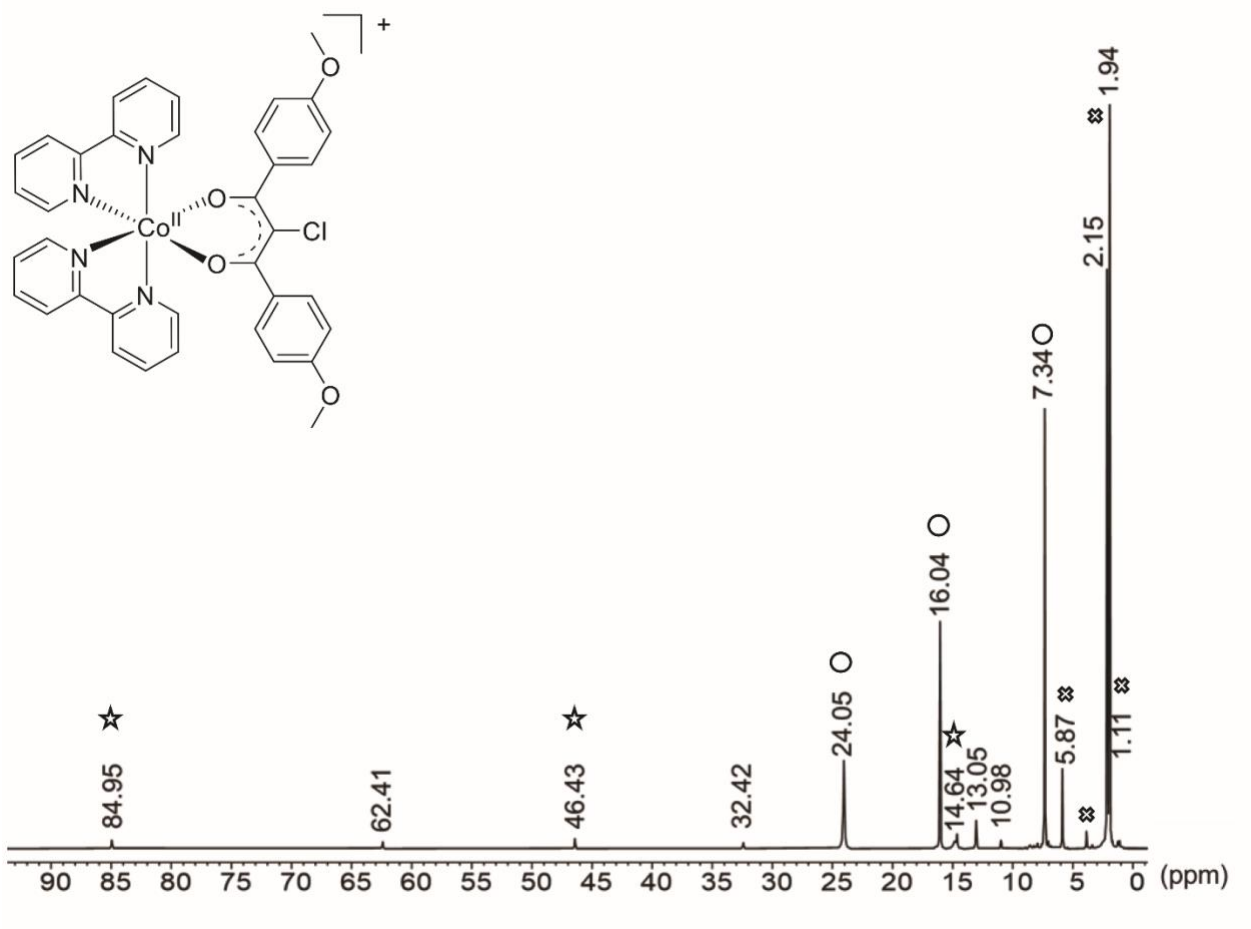


**Fig S9.** $^{1}$H NMR of **10** in $CD_3CN$. The signals marked with an open circle correspond to the coordinated diketonate ligand in **10**. Signals marked with a star indicate those from $[(bpy)_3Co](ClO_4)_2$ (**11**). Residual solvent signals are indicated with (X).

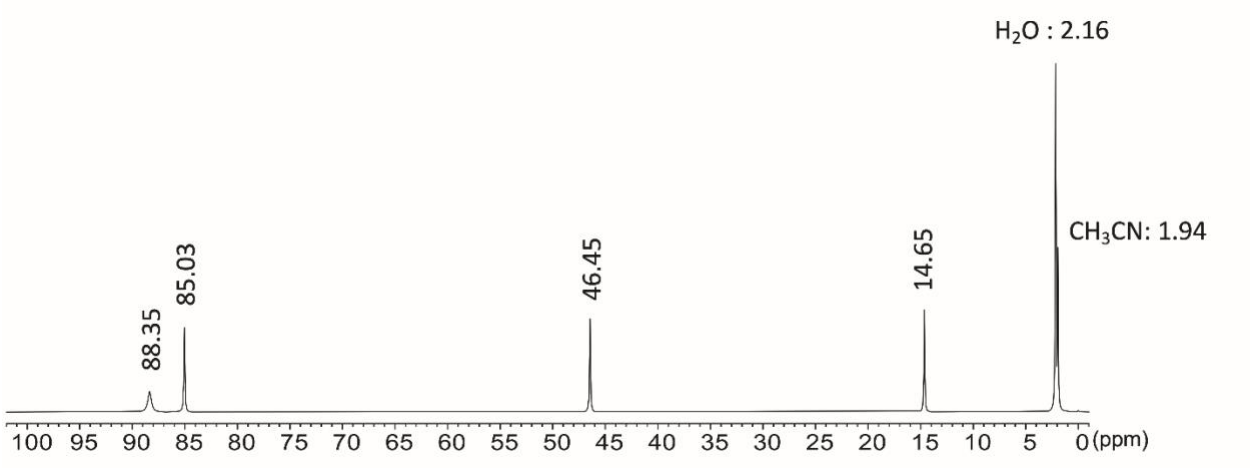


**Fig S10.** $^{1}$H NMR of $[(bpy)_3Co](ClO_4)_2$ (**11**) in $CD_3CN$.

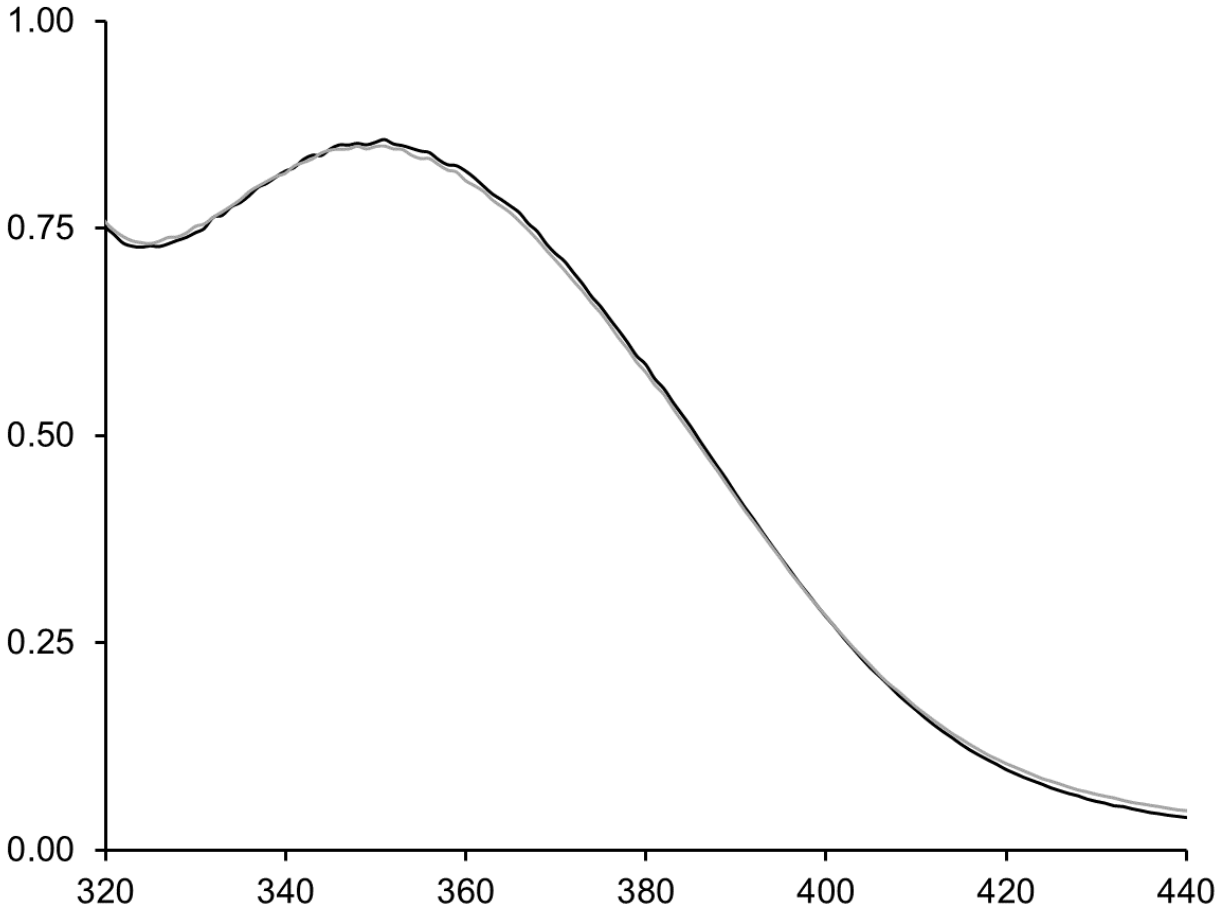


**Fig S11.** UV-Vis spectrum of **8** (black) in $CH_3CN$. The spectrum in gray is for the same solution after exposure to air in the dark for 20 hours.

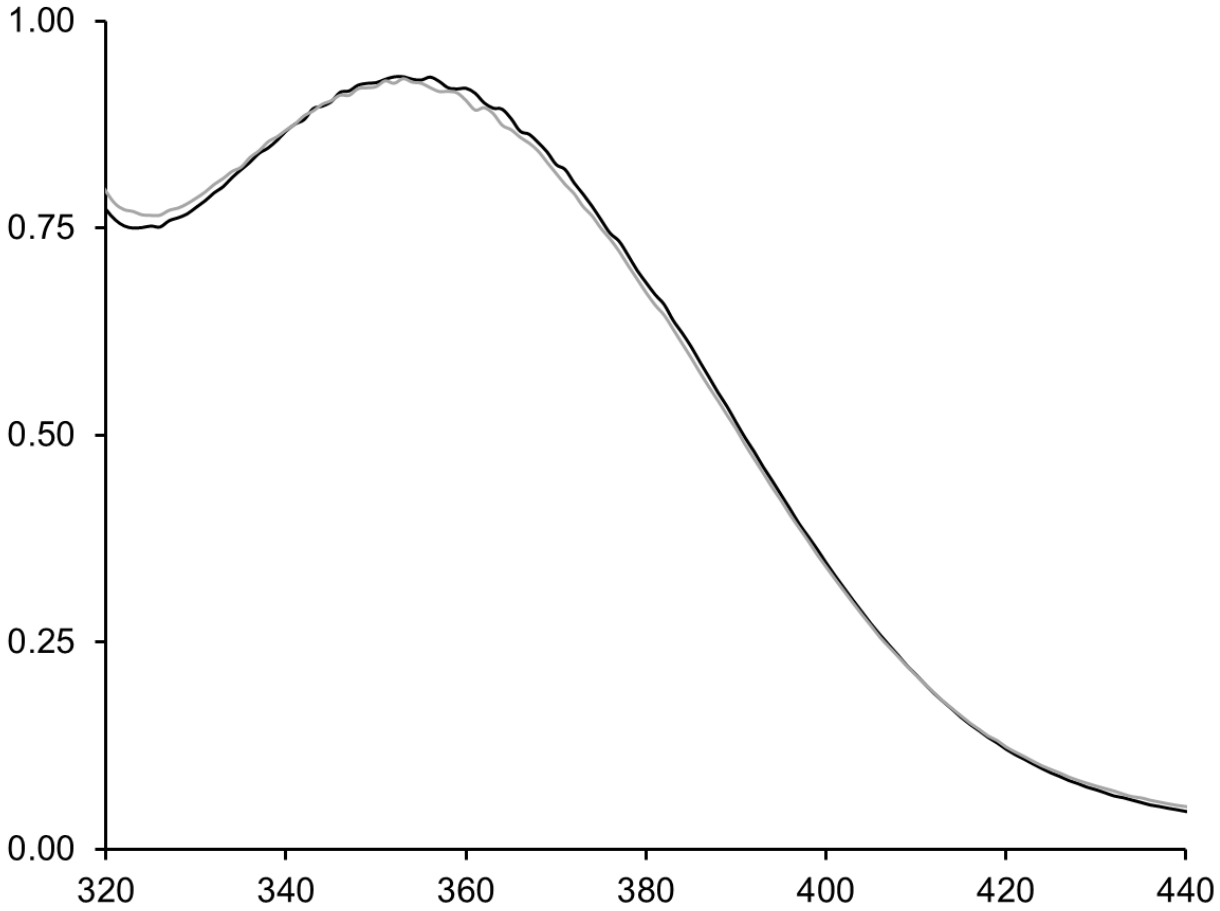


**Fig S12.** UV-Vis spectrum of **9** (black) in $CH_3CN$. The spectrum in gray is for the same solution after exposure to air in the dark for 20 hours.

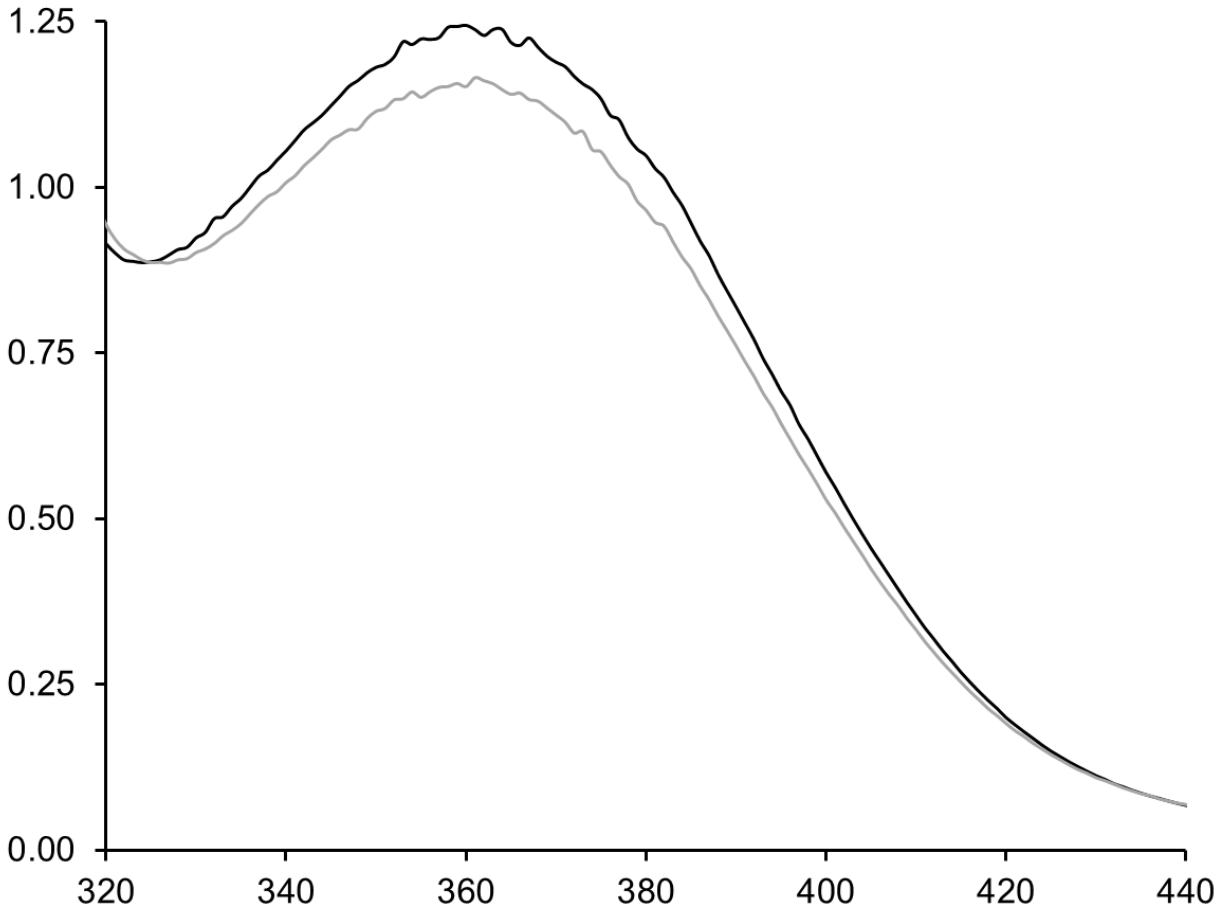


**Fig S13.** Absorption spectrum of **10** (black) in $CH_3CN$. The spectrum in gray is for the same solution after exposure to air in the dark for 20 hours.

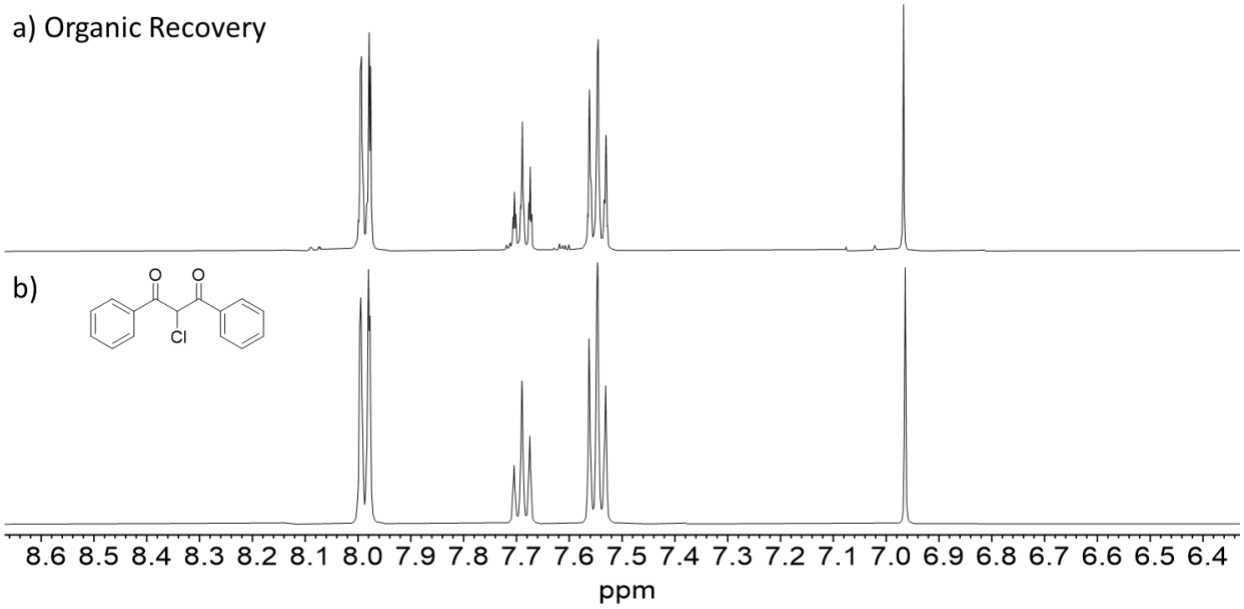


**Fig S14.** $^{1}H$ NMR spectra in $CD_3CN$ from: a) The isolated organic products from illumination of **8** at 350 nm for 20 hours under $N_2$. b) 2-chloro-1,3-diphenyl-1,3-propandione.

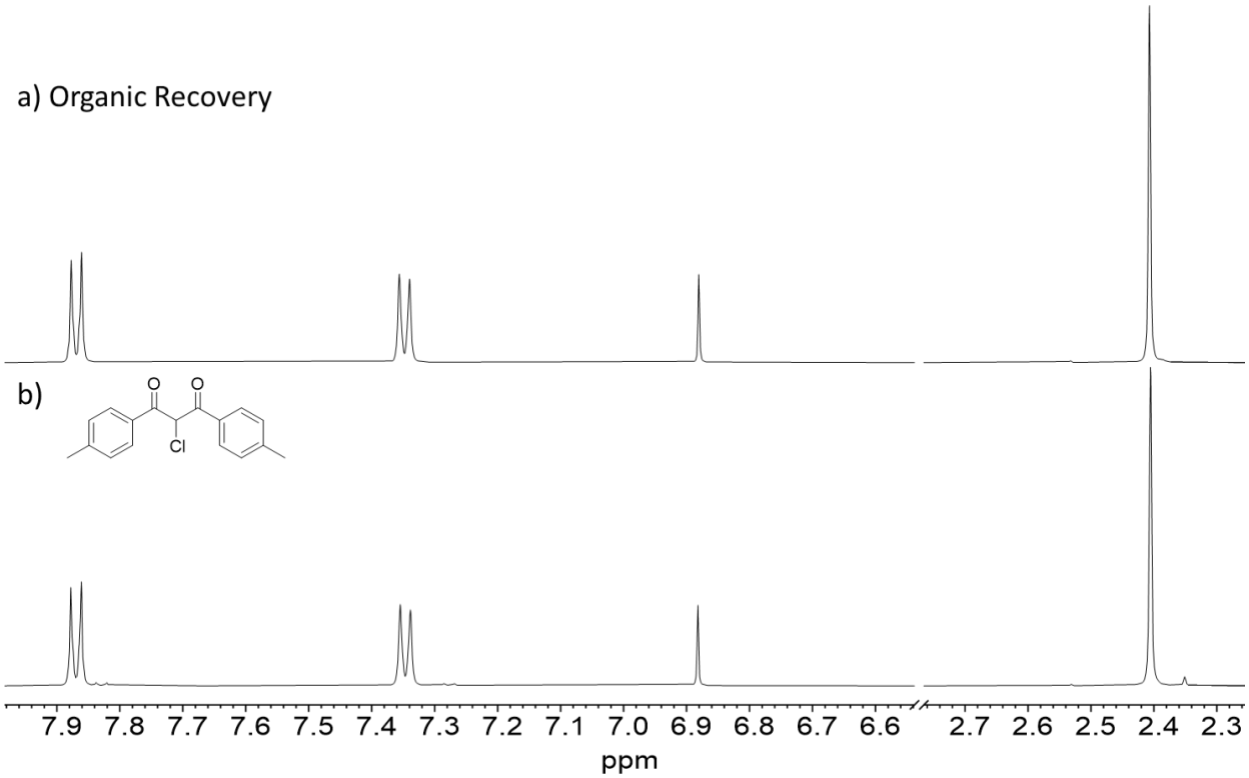


**Fig S15.** $^{1}H$ NMR spectra in $CD_3CN$ from: a) The isolated organic products from illumination of **9** at 350 nm for 20 hours under $N_2$. b) 2-chloro-1,3-bis(4-methylphenyl)-1,3-propanedione.

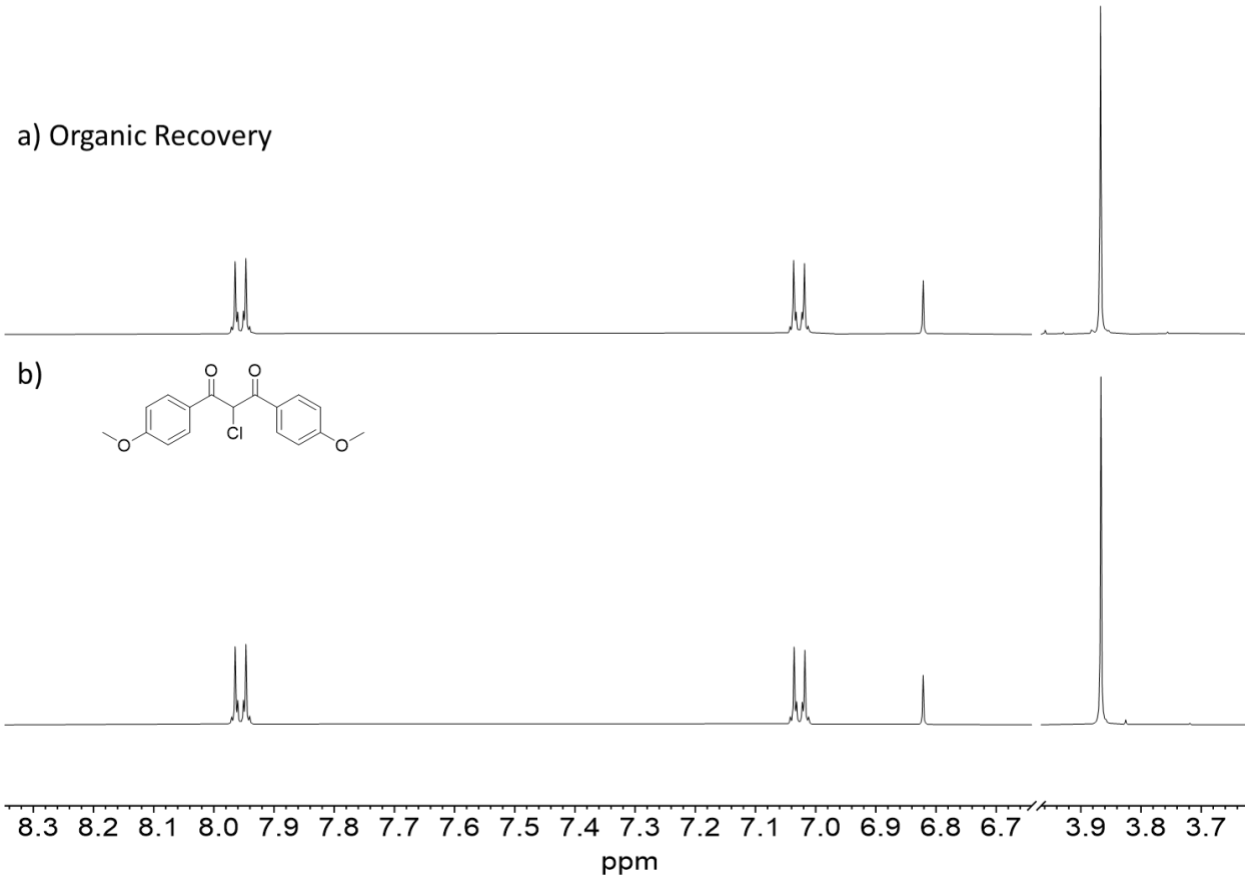


**Fig S16.** $^{1}H$ NMR spectra in $CD_3CN$ from: a) The isolated organic products from illumination of **10** at 350 nm for 20 hours under $N_2$. b) 2-chloro-1,3-bis(4-methoxyphenyl)-1,3-propandione.

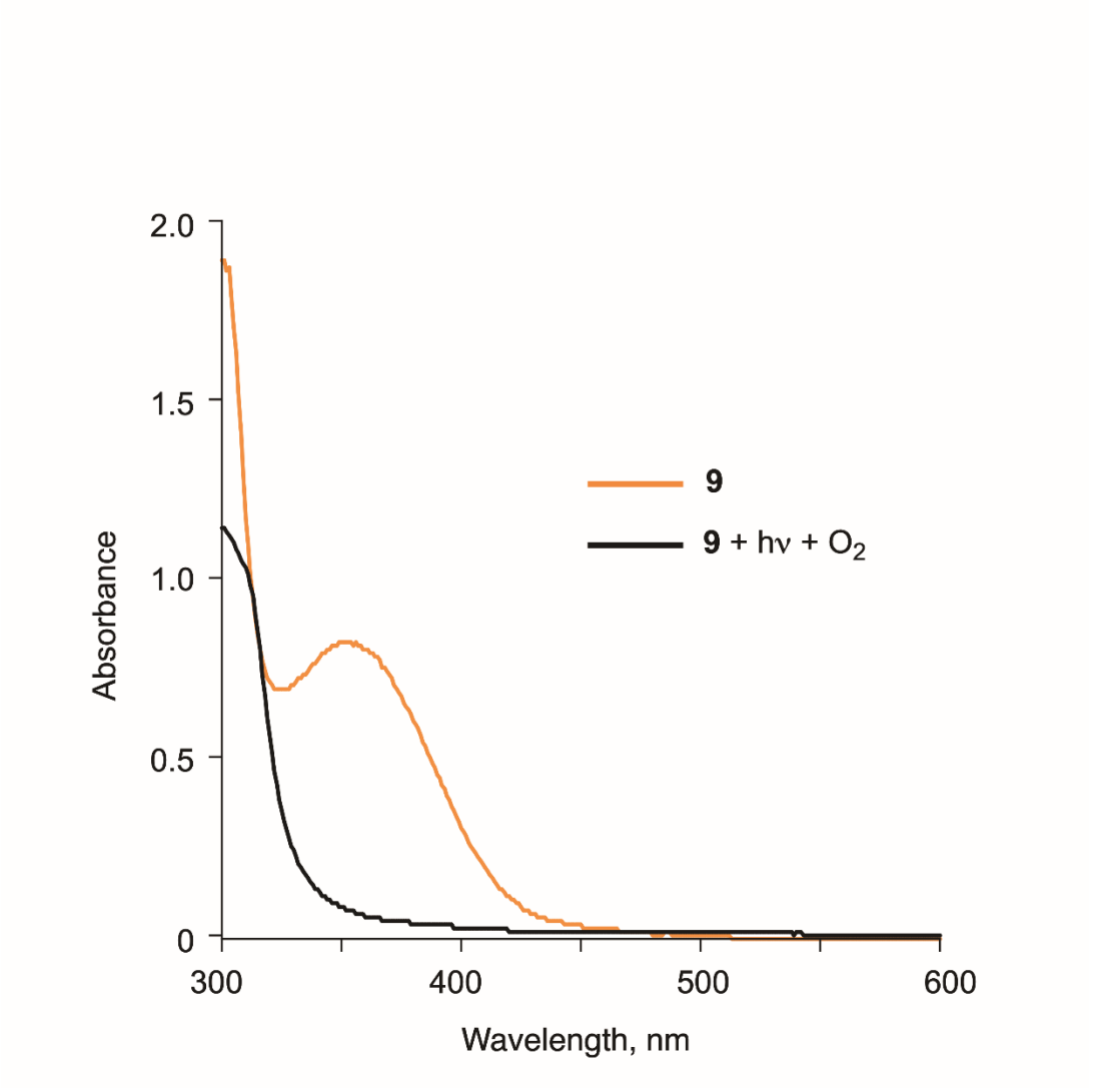


**Fig S17.** Absorption spectral changes upon illumination of **9** in $O_2$-purged $CH_3CN$ at 350 nm.

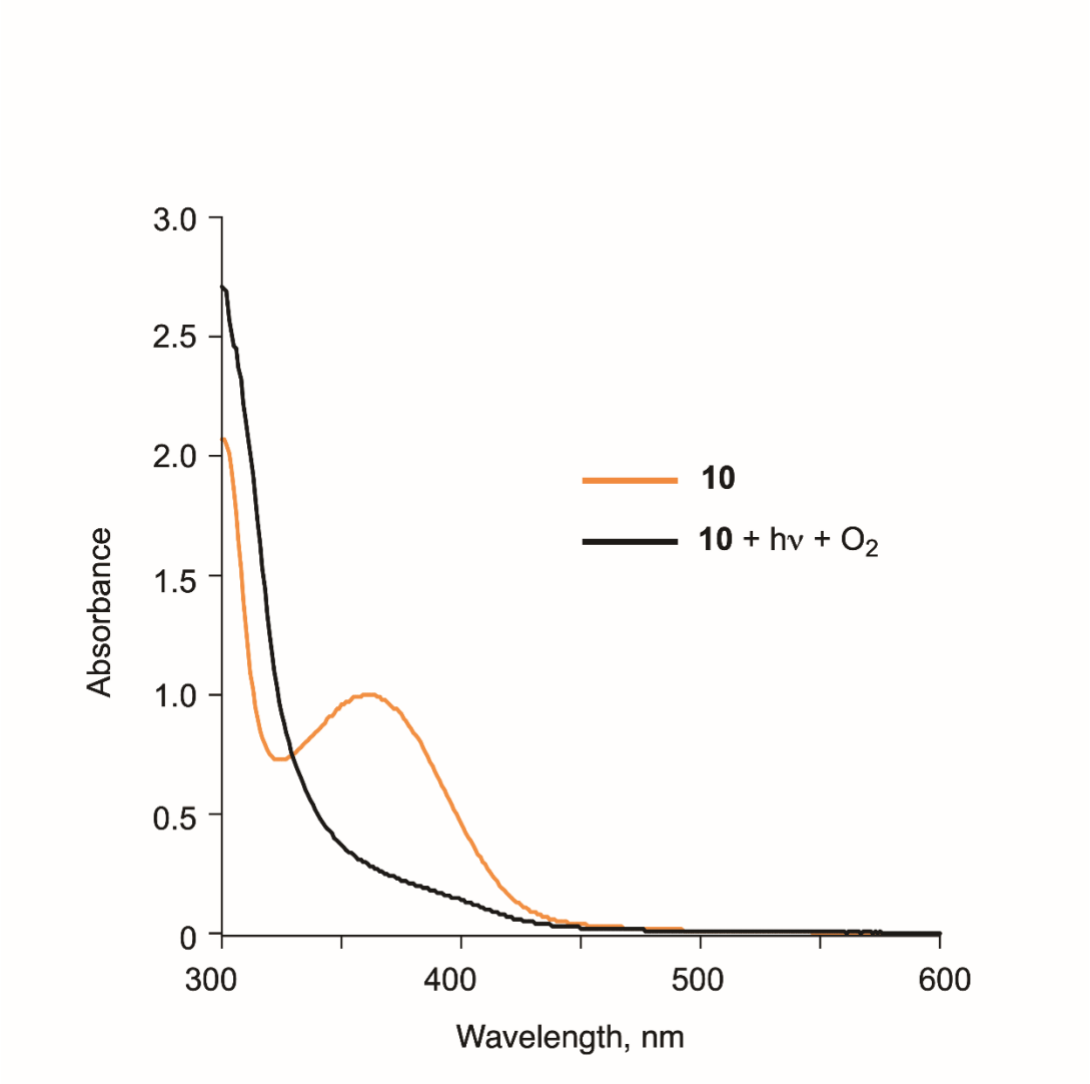


**Fig S18.** Absorption spectral changes upon illumination of **10** in $O_2$-purged $CH_3CN$ at 350 nm.

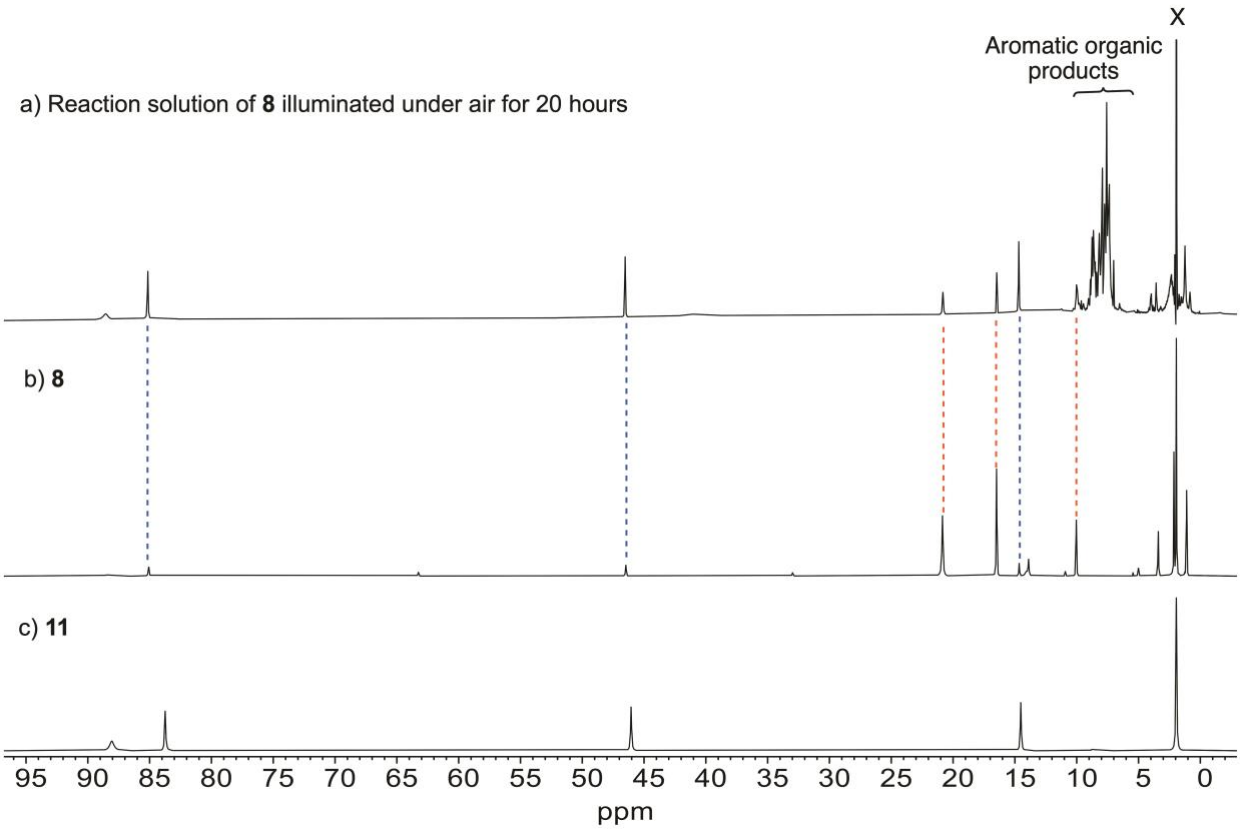


**Fig S19.** $^{1}$H NMR studies of the UV-light induced $O_2$ reactivity of **8** in $CD_3CN$ (residual solvent signal designated by X). a) Product mixture for an $O_2$-purged $CH_3CN$ solution of **8** after illumination with 350 nm lamps for 20 hours; b) $^{1}$H NMR spectrum of **8**. The change in the relative intensity of the signals for **8** and $[(bpy)_3Co](ClO_4)_2$ (**11**), designated by red and blue dashed lines, respectively, and the appearance of signals for free aromatic organic products, provide evidence for the light-driven diketonate reactivity. c) $^{1}$H NMR of $[(bpy)_3Co](ClO_4)_2$ (**11**) in $CD_3CN$. The slight shift in the signals of this compound at ~46 and ~84 ppm in the sample containing **8** (spectrum b)) is attributed to the presence paramagnetic character of the compounds.

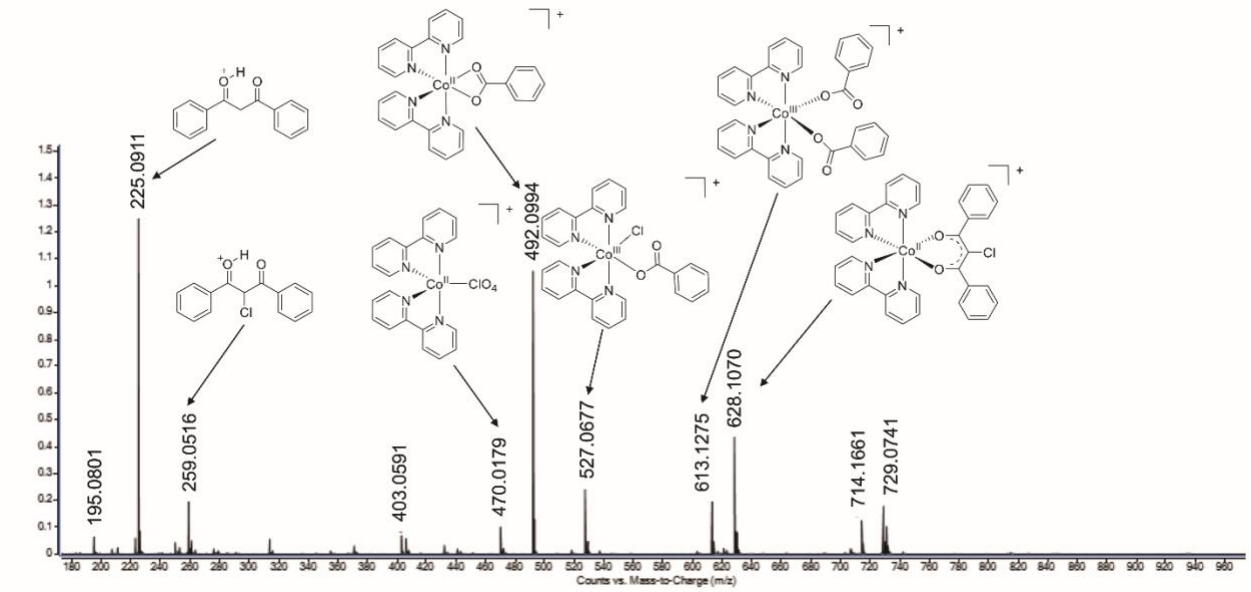


**Fig S20.** ESI-MS of an $O_2$-purged $CH_3CN$ solution of **8** after illumination at 350 nm for 20 hours.

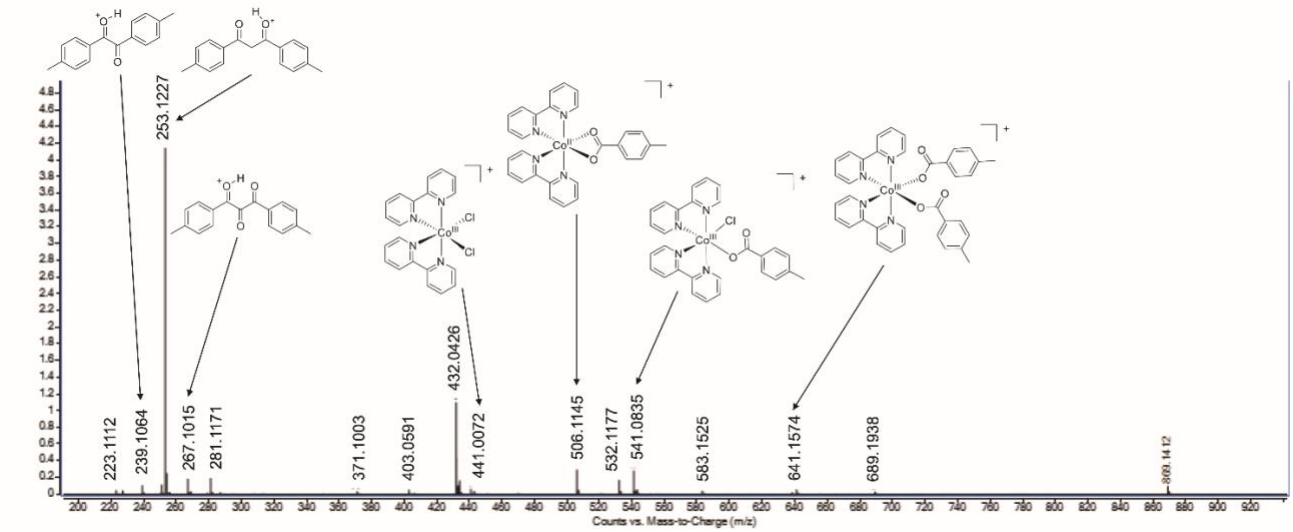


**Fig S21.** ESI-MS of an $O_2$-purged $CH_3CN$ solution of **9** after illumination at 350 nm for 20 hours.

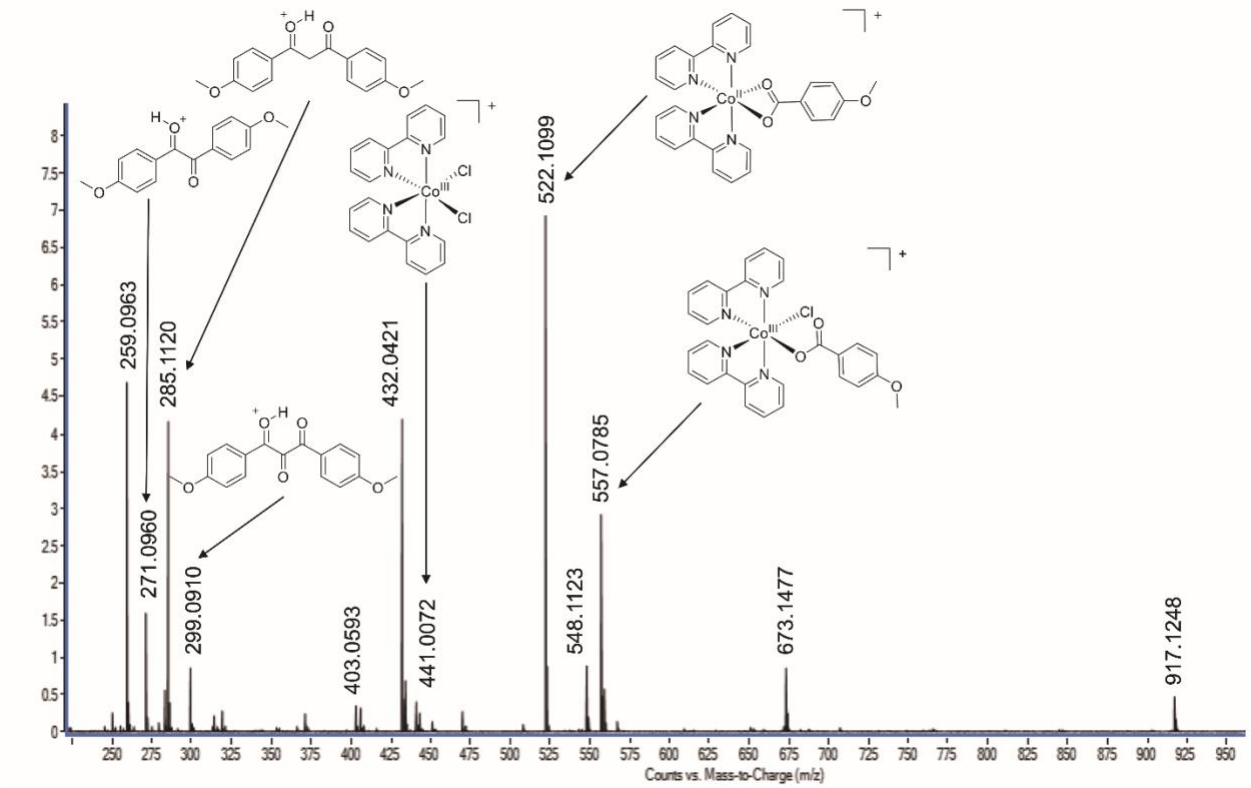


**Fig S22.** ESI-MS of an $O_2$-purged $CH_3CN$ solution of **10** after illumination at 350 nm for 20 hours.

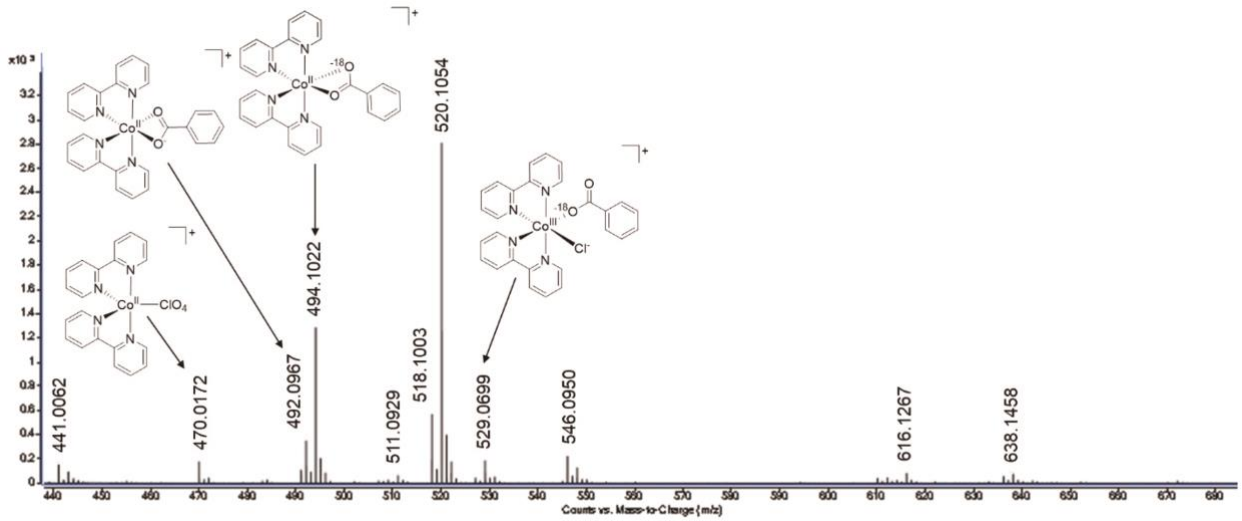


**Fig S23**. ESI-MS of an $CH_3CN$ solution of **8** illuminated at 350 nm under $^{18}O_2$ for 20 hours. $^{18}O$ incorporation is indicated by comparison of the isotope patterns for $[(bpy)_2Co(^{18}OOCPh)]^+$ (*m/z* 494.1022) and $[(bpy)_2Co(O_2CPh)]^+$ (*m/z* 492.0967).

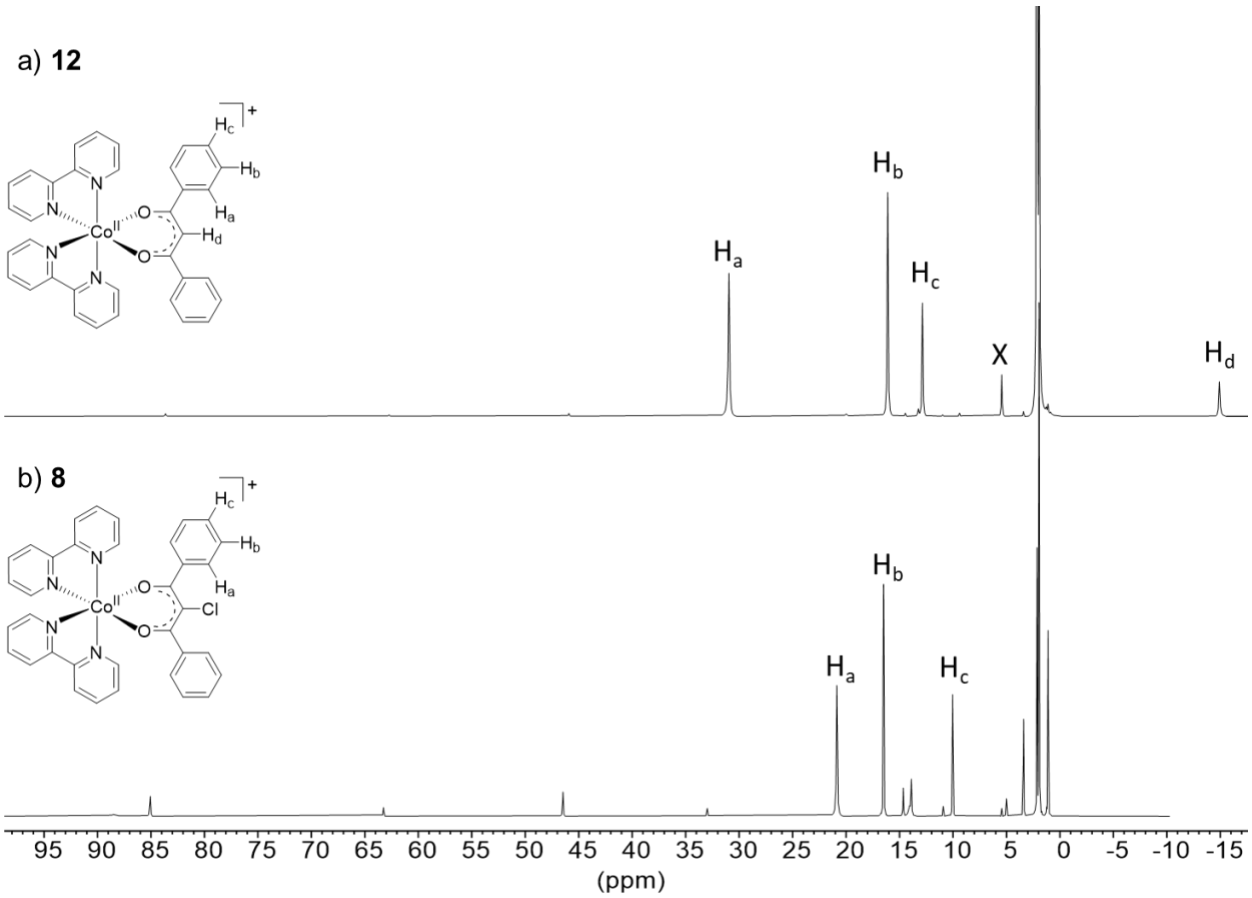


**Fig S24**. a) $^{1}$H NMR of **12** in $CD_3CN$. A residual solvent signal ($CH_2Cl_2$) is indicated with (X) in the spectrum of **12**; b) $^{1}$H NMR of **8** in $CD_3CN$.

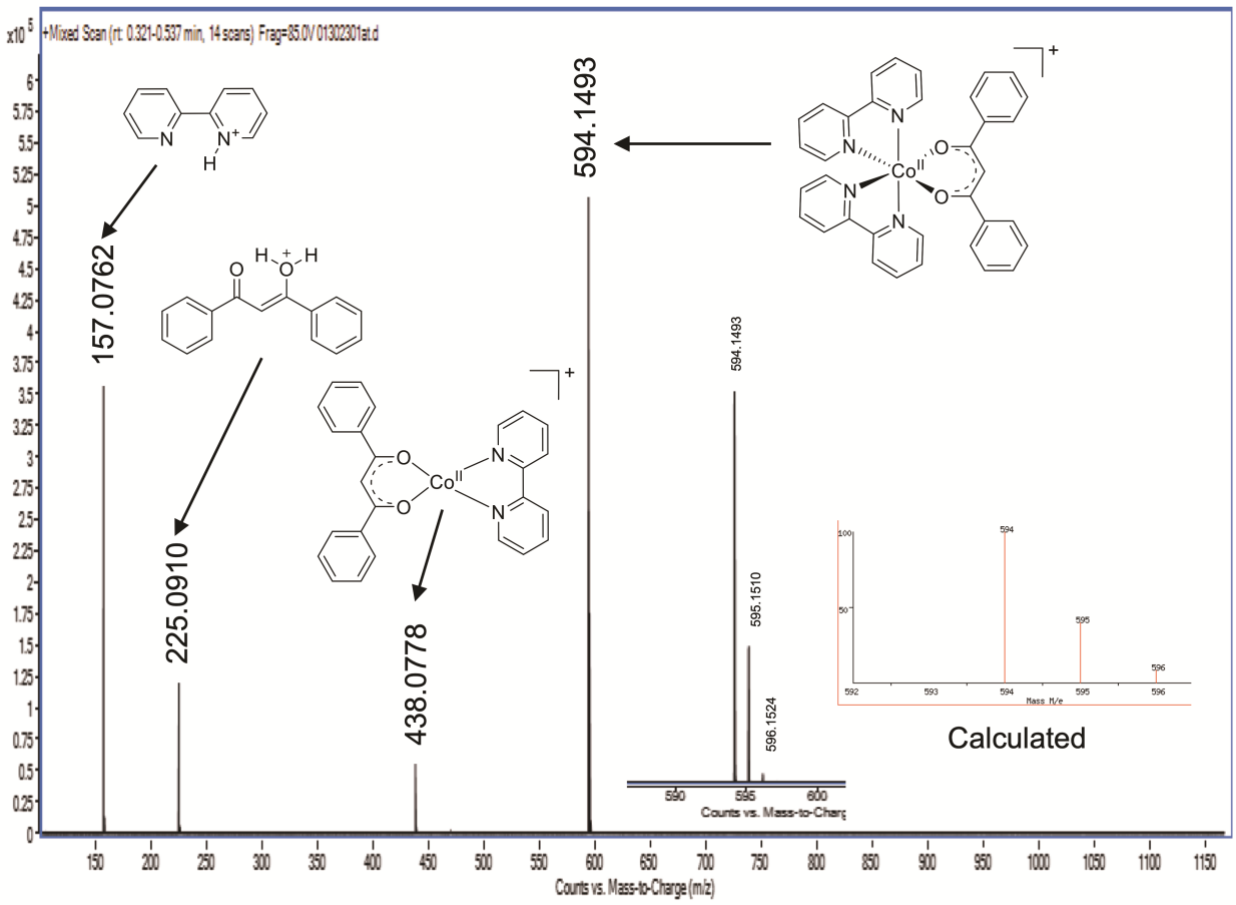


**Fig S25**. ESI-MS of **12** in $CH_3CN$.

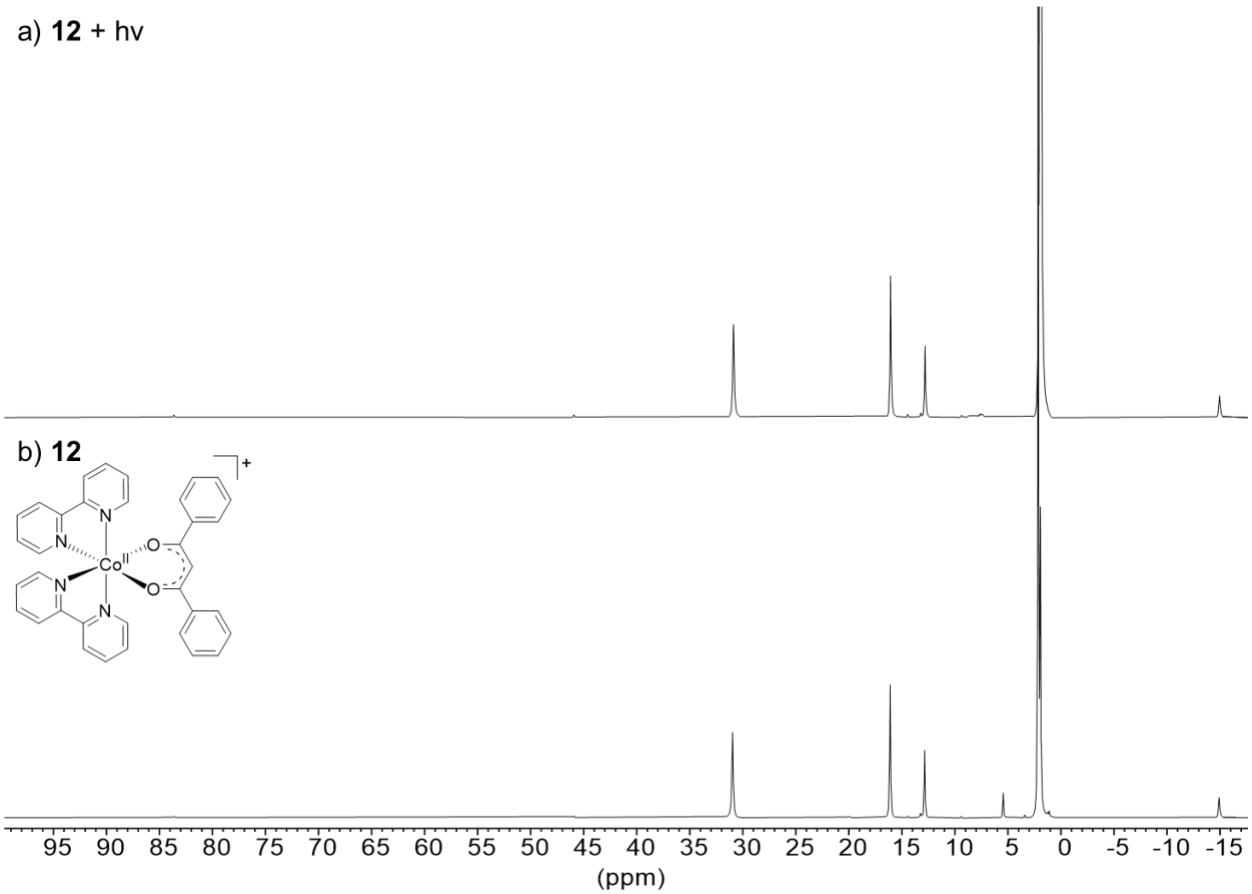


**Fig S26**. a) $^{1}$H NMR of **12** after illumination at 350 nm in $CD_3CN$. b) **12** before illumination.

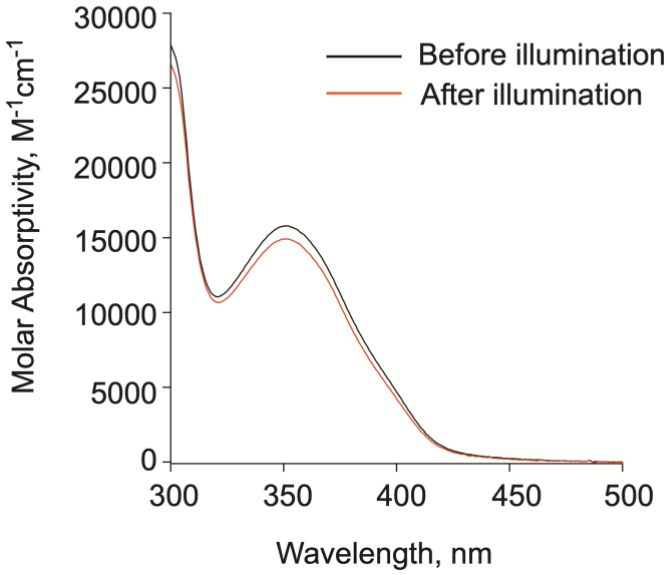


**Fig S27**. Absorption spectral features of **12** in acetonitrile before and after illumination of an $O_2$ purged solution at 350 nm.

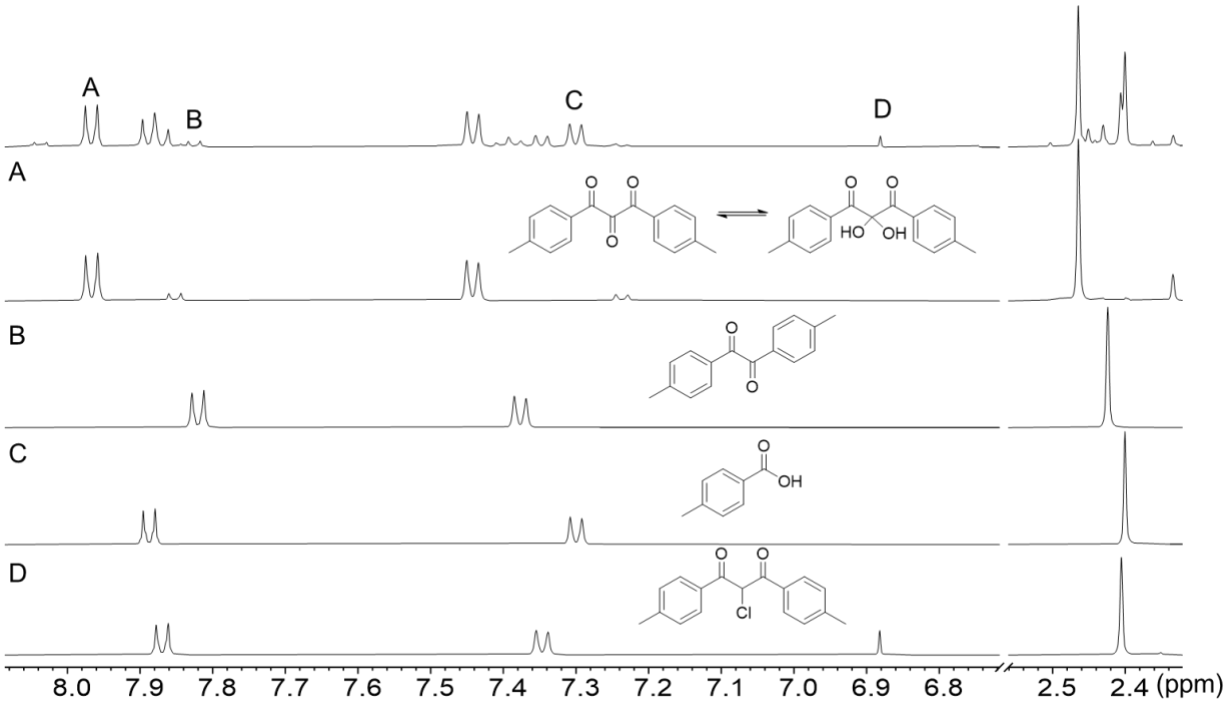


**Fig S28.** $^{1}$H NMR of isolated organic products from the illumination of **9** in $O_2$-purged $CH_3CN$ with 350 nm for 20 hours (top) compared to the $^{1}$H NMR of organic products (A-D). Resonances that can be used to identify a specific product are marked with A-D. Spectra collected in $CD_3CN$.

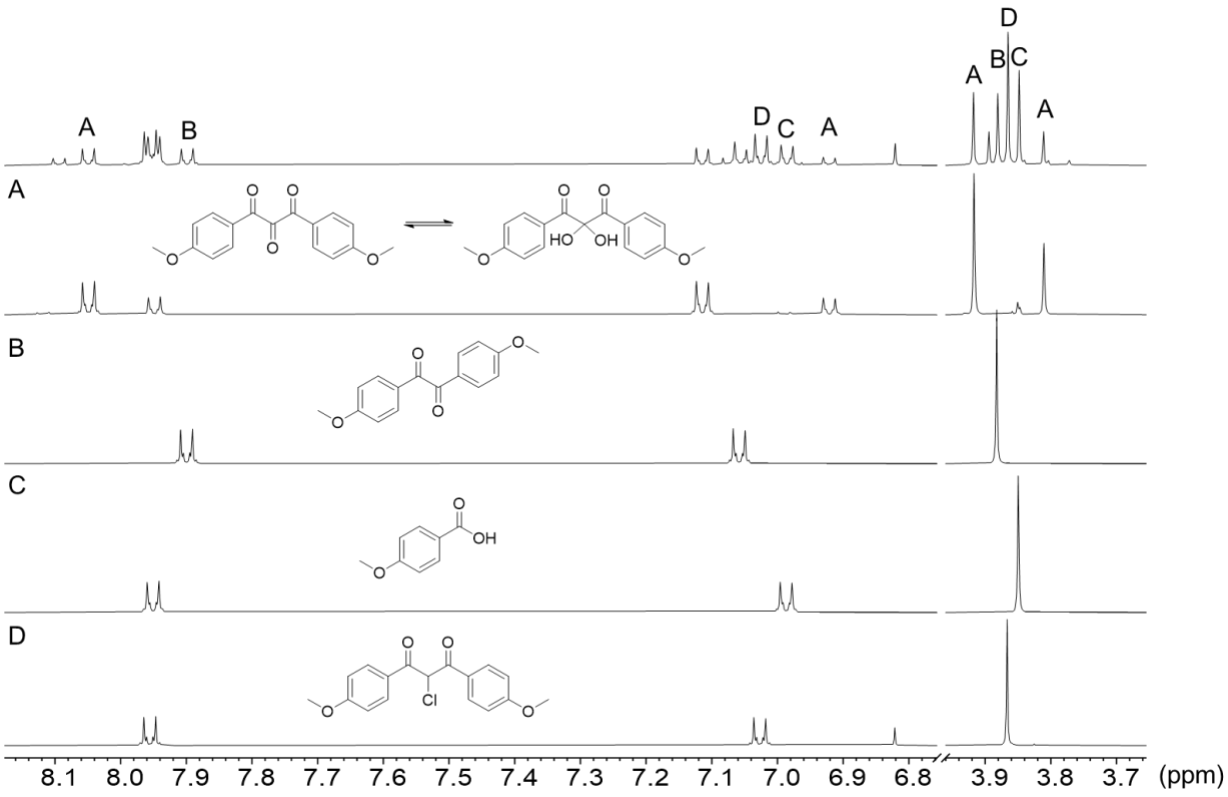


**Fig S29.** $^{1}$H NMR of isolated organic products from the illumination of **10** in $O_2$-purged $CH_3CN$ with 350 nm for 20 hours (top) compared to the $^{1}$H NMR of organic products (A-D). Resonances that can be used to identify a specific product are marked with A-D. Spectra collected in $CD_3CN$.

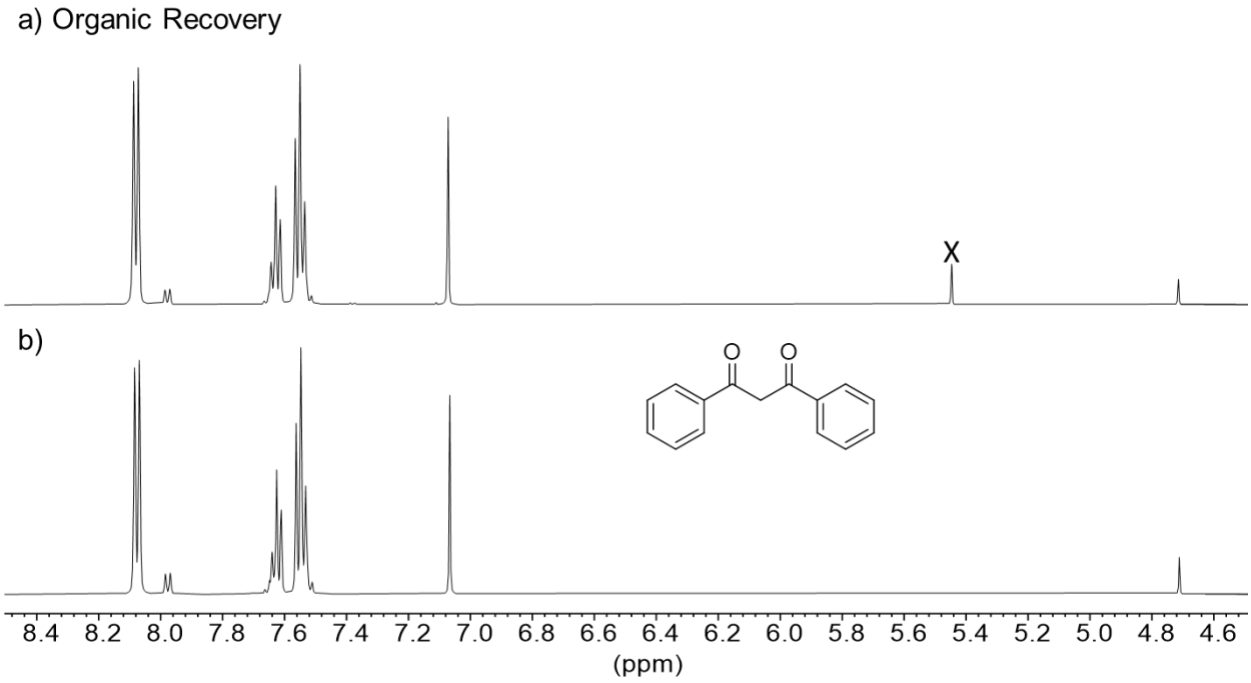


**Fig S30**. $^{1}$H NMR of a) isolated organic products from the illumination of **12** in $O_2$-purged with 350 nm for 20 hours and b) dibenzoylmethane dissolved in $CD_3CN$. A residual solvent signal ($CH_2Cl_2$) is indicated with (X) in the spectrum of the sample derived from **12**.

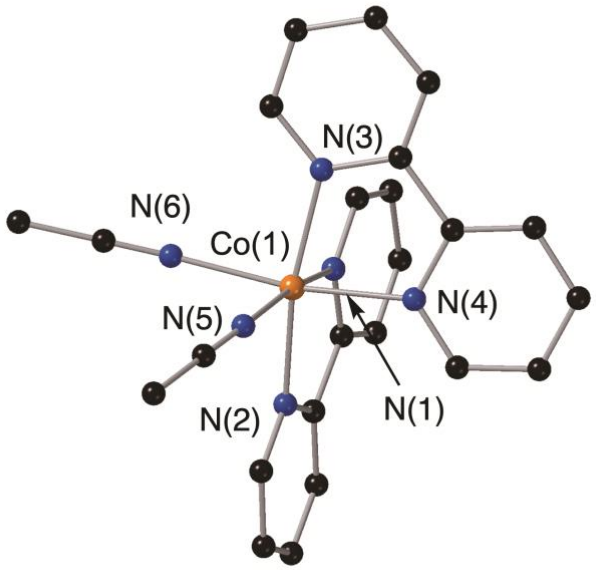


**Fig S31.** Representation of the cationic portion of **13**.

**Table S4.** Selected bond distances (Å) for **13**

| | **13** |
|---|---|
| Co(1)-N(1) | 2.1245(14) |
| Co(1)-N(2) | 2.1228(14) |
| Co(1)-N(3) | 2.1198(15) |
| Co(1)-N(4) | 2.1246(14) |
| Co(1)-N(5) | 2.1358(15) |
| Co(1)-N(6) | 2.1356(16) |

**Table S5.** Selected bond angles (deg) for **13**

| | **13** |
|---|---|
| N(1)-Co(1)-N(2) | 77.20(5) |
| N(1)-Co(1)-N(3) | 94.48(5) |
| N(1)-Co(1)-N(4) | 88.68(5) |
| N(1)-Co(1)-N(5) | 169.70(6) |
| N(1)-Co(1)-N(6) | 94.04(6) |
| N(2)-Co(1)-N(3) | 168.65(5) |
| N(2)-Co(1)-N(4) | 94.69(6) |
| N(2)-Co(1)-N(5) | 92.84(6) |
| N(2)-Co(1)-N(6) | 95.02(6) |
| N(3)-Co(1)-N(4) | 77.22(6) |
| N(3)-Co(1)-N(5) | 95.74(6) |
| N(3)-Co(1)-N(6) | 93.24(6) |
| N(4)-Co(1)-N(5) | 94.82(6) |
| N(4)-Co(1)-N(6) | 170.27(6) |

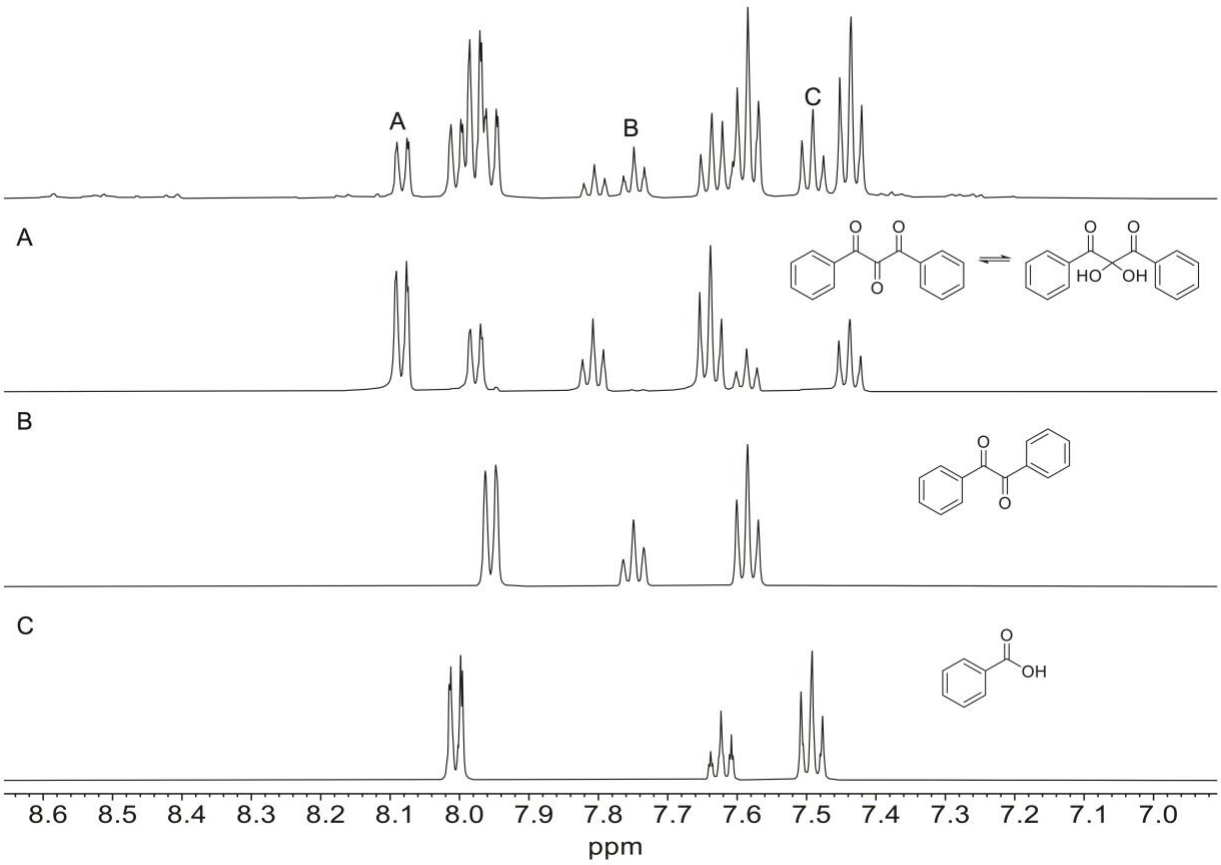


**Fig S32**. $^{1}$H NMR of isolated organic products from the reaction of **13** with 1,3-diphenylpropanetrione with NaOCl in $CH_3CN$. $O_2$ was bubbled into the solution of **13** for two minutes. The isolated products (top) are compared to the $^{1}$H NMR of organic standards (A-C). Spectra collected in $CD_3CN$.

**Fig S33.** Dark red-brown solution generated upon bubbling of $O_2$ through a $CH_3CN$ solution of **13** for 8 h.

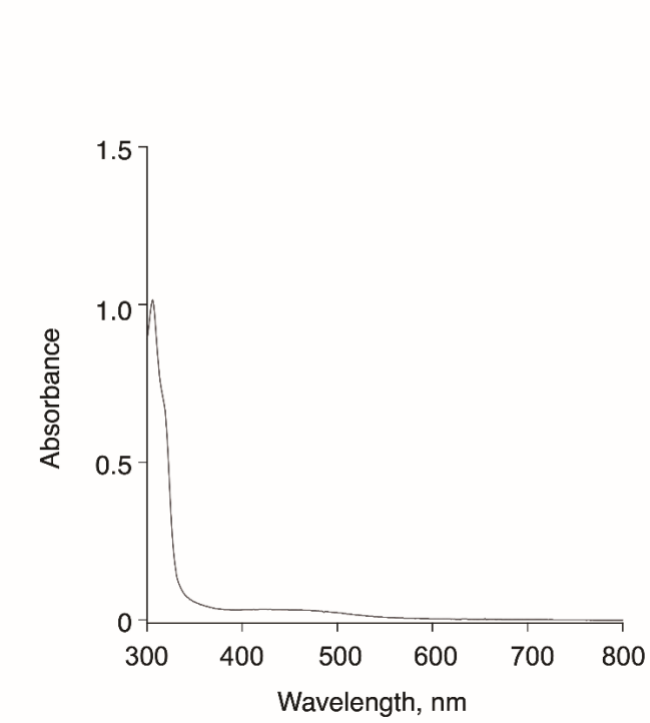


**Fig S34.** Absorption spectrum of **13** ($2.94 \times 10^{-5}$ M) in $CH_3CN$ after bubbling with $O_2$ for 8 h.

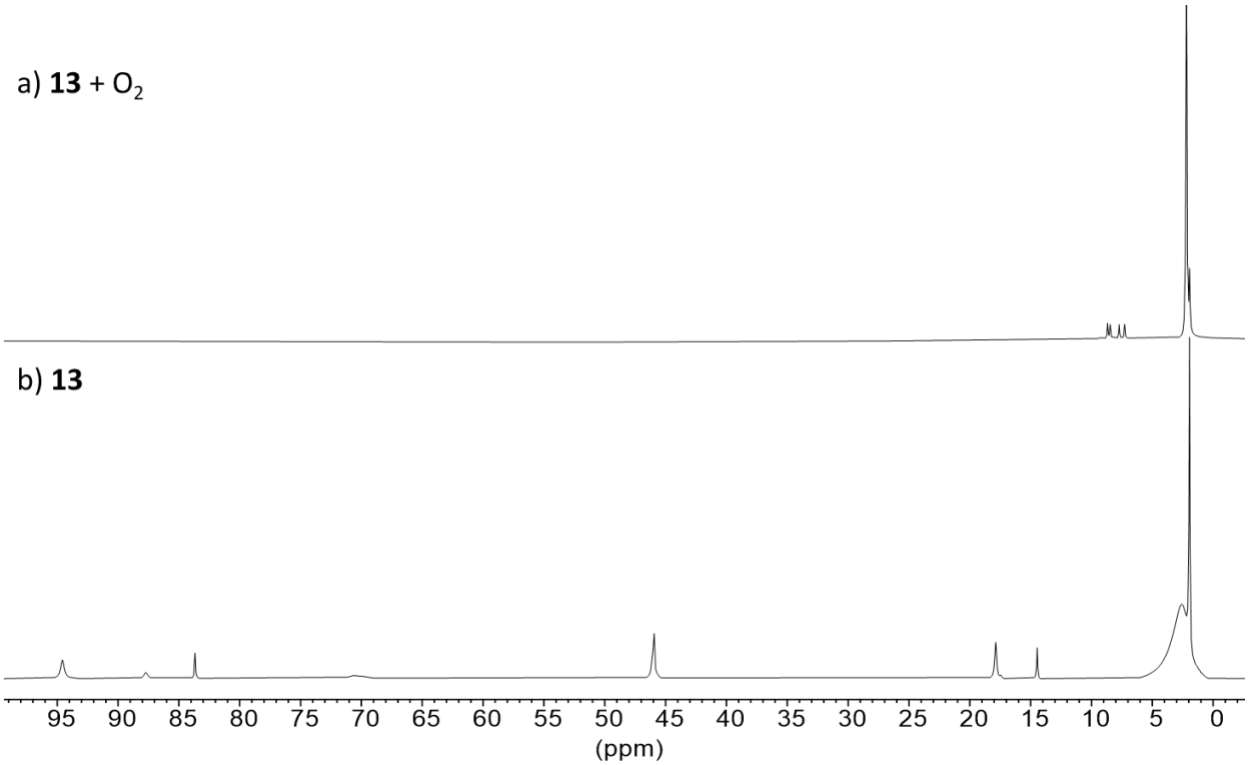


**Fig S35.** $^{1}$H NMR spectra in $CD_3CN$ of a) **13** + $O_2$ for 8 h and b) **13**.

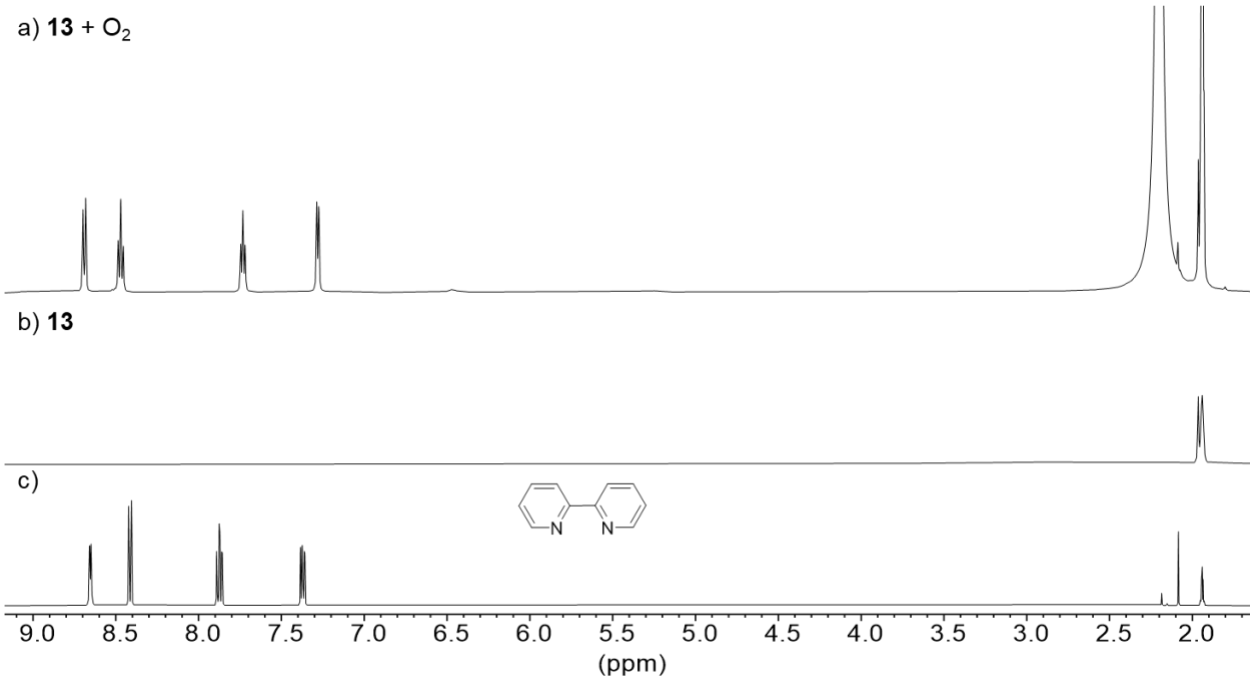


**Fig S36.** $^{1}$H NMR spectra in $CD_3CN$ of a) **13** + $O_2$ for 8 h; b) **13** and c) 2,2'-bipyridine.

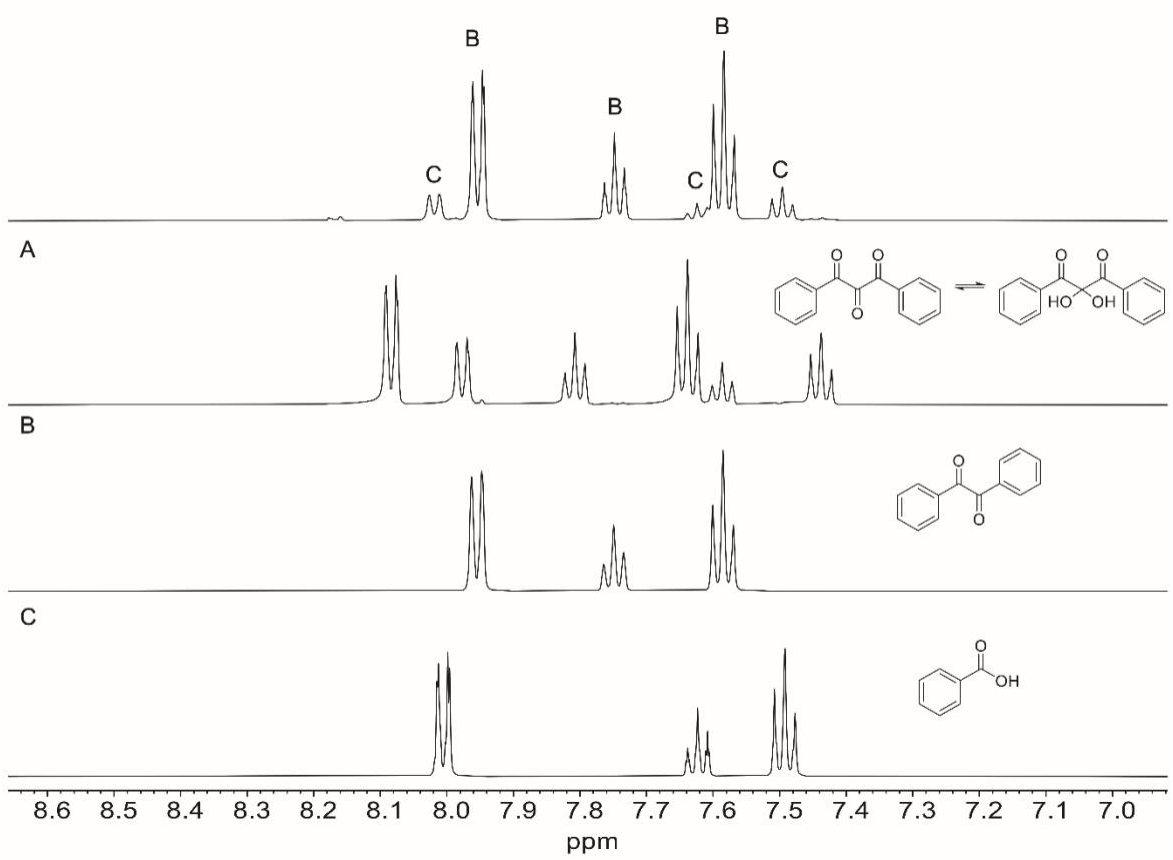


**Fig S37**. $^{1}$H NMR of isolated organic products from the reaction of **13** with 1,3-diphenylpropanetrione with NaOCl in $CH_3CN$. $O_2$ was bubbled into the solution of **13** for 8 h. This resulted in the solution becoming dark red-brown (Fig S33). The trione and NaOCl were then added. The isolated products (top) are compared to the $^{1}$H NMR of pure organic products (A-C). Spectra collected in $CD_3CN$

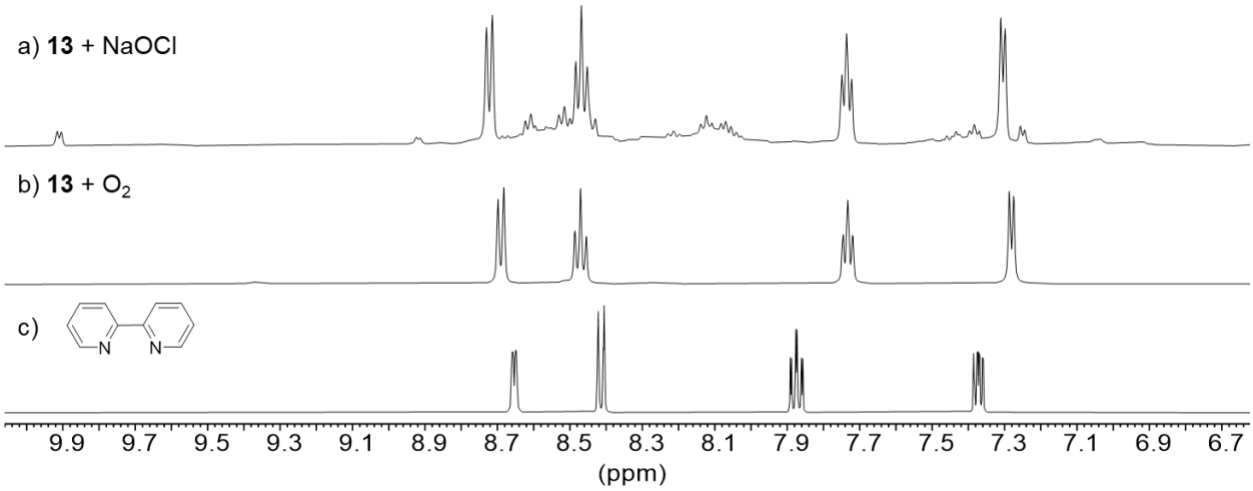


**Fig S38**. $^{1}H$ NMR features in the aromatic region of $CD_3CN$ solutions of **13** upon treatment with stoichiometric NaOCl (a), or upon extended exposure to $O_2$ (b). Distinct chemical shifts from free bipyridine c) suggest the formation of bpy-ligated Co(III) species.

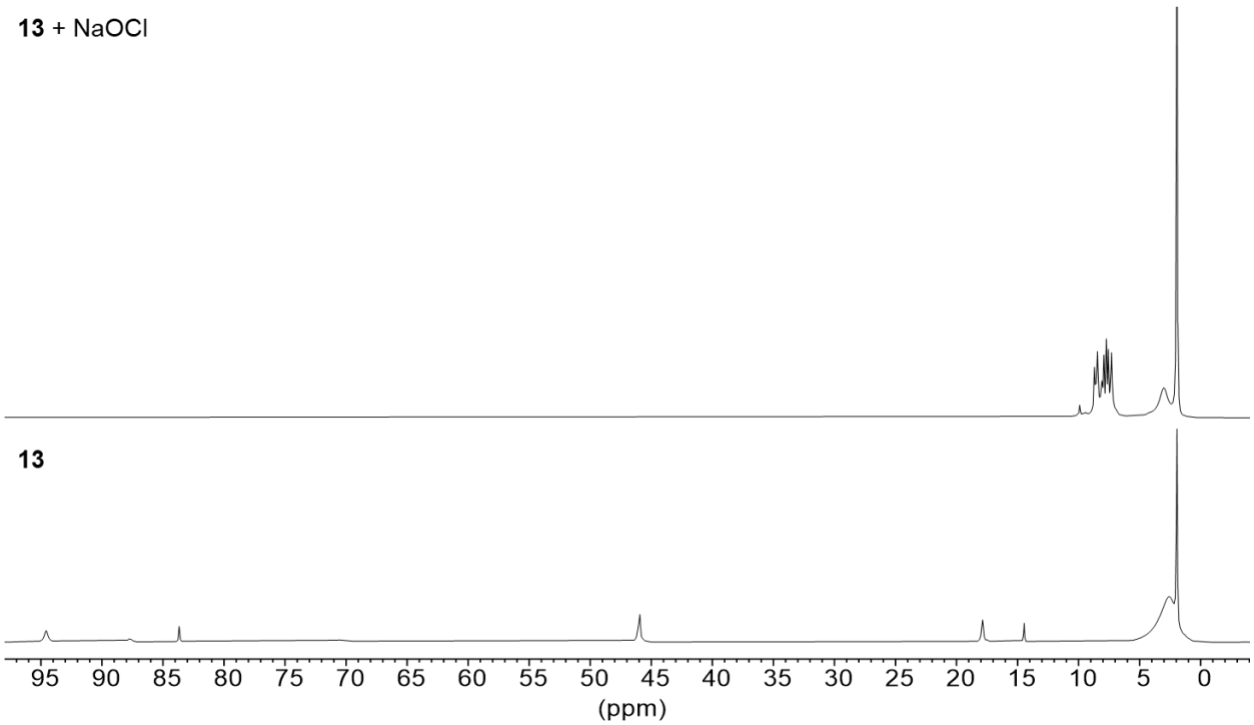


**Fig S39.** $^{1}$H NMR spectra in $CD_3CN$ of a) **13** + NaOCl and b) **13**.